REPORT DOCUMENTATION PAGE

Form Approved OMB No. 0704-0188

1. AGENCY USE ONLY (Leave blank)	2. REPORT DATE	3. REPORT TYPE AND DATES COVERED
	30 Sep. 1999	Final Report

4. TITLE AND SUBTITLE

Development of Computational Techniques for Studying Interpenetrating Plasma Flows and Microwave Impulse

5. FUNDING NUMBERS

F61775-98-WE124

6. AUTHOR(S)

Professor Evgeniy Leonidovich Stupitsky

7. PERFORMING ORGANIZATION NAME(S) AND ADDRESS(ES)

High Energy Density Research Center (HEDRC)
Izhorskaya 13/19
Moscow 127412
Russia

8. PERFORMING ORGANIZATION REPORT NUMBER

N/A

9. SPONSORING/MONITORING AGENCY NAME(S) AND ADDRESS(ES)

EOARD
PSC 802 BOX 14
FPO 09499-0200

10. SPONSORING/MONITORING AGENCY REPORT NUMBER

SPC 98-4079

11. SUPPLEMENTARY NOTES

12a. DISTRIBUTION/AVAILABILITY STATEMENT

Approved for public release; distribution is unlimited.

12b. DISTRIBUTION CODE

A

13. ABSTRACT (Maximum 200 words)

This report results from a contract tasking High Energy Density Research Center (HEDRC) as follows: The contractor will simulate the merging plasma ensemble as three fluids- one for the ion component of each plasma and one for a single common electron fluid. Issues which must be successfully addressed include conservation of momentum and energy, accommodating widely varying time scales for different processes, and avoidance of numerical artifacts such as numerical diffusion. They will evaluate and determine the most effective algorithms.

19991209 074

14. SUBJECT TERMS

EOARD, High Power Microwaves, Plasma Physics, Simulation

15. NUMBER OF PAGES

36

16. PRICE CODE

N/A

17. SECURITY CLASSIFICATION OF REPORT	18. SECURITY CLASSIFICATION OF THIS PAGE	19. SECURITY CLASSIFICATION OF ABSTRACT	20. LIMITATION OF ABSTRACT
UNCLASSIFIED	UNCLASSIFIED	UNCLASSIFIED	UL

NSN 7540-01-280-5500

Standard Form 298 (Rev. 2-89)
Prescribed by ANSI Std. 239-18
298-102

DTIC QUALITY INSPECTED 4

# of Work "*Development of Computation Techniques for Studying Interpenetrating Plasma Flows and Microwave Impulse*", Contract number F61775-98-WE124 SPC-98-4079

1. Introduction

In the final report, given no consideration to the modern achievements in the problem under study and to the analysis of a number of physical processes to justify the problem statement that are given in detail in reports of Items 2-4, we present only those sections in which the formulae are directly used in two-dimensional code. The algorithm structure, program code and its description, and also some results of calculations are presented in appendix.

2. Calculation Methods of Electron and Ion Temperatures and Charge Composition

Since in kinetic equations for calculation of charge composition and in the equation for electron temperature the terms connected with non-elastic processes have the same structure, clearly the differential algorithm should be built from the integration of blocks that calculate their. In three-speed approximation the system of ionization-temperature equations takes the form:

$$\frac{\partial n_{1z}}{\partial t} + div(n_{1z} * \vec{V}_1) = S_{1z} \tag{2.1}$$

$$\frac{\partial n_{2z}}{\partial t} + div(n_{2z} * \vec{V}_2) = S_{2z} \tag{2.2}$$

$$Z=0,1,2,...Z_m$$

$$\frac{\partial n_e}{\partial t} + div(n_e * \vec{V}_e) = S_e \tag{2.3}$$

$$\frac{3}{2} * n_1 * \frac{dT_1}{dt} + n_1 * T_1 * div\vec{V}_1 = Q_1 \tag{2.4}$$

$$\frac{3}{2} * n_2 * \frac{dT_2}{dt} + n_2 * T_2 * div\vec{V}_2 = Q_2 \tag{2.5}$$

$$\frac{3}{2} * n_e * \frac{dT_e}{dt} + n_e * T_e * div\vec{V}_e = div(\lambda_e \nabla T_e) + S_{ee} + Q_e \tag{2.6}$$

Calculation has shown that ion contribution to variation of electron density is infinitesimally small in comparison with electrons themselves. Therefore, the velocities S_{1z} for in-

coming flow and S_{2z} for reflected flow are defined by collisions of ions with electrons and by the overcharging processes between ions of counter flows.

$$S_{1z} = (n_{1z-1} * n_e * j_{z-1e} - n_{1z} * n_e^2 * j_{ez}) - (n_{1z} * n_e * j_{ze} - n_{1z+1} * n_e^2 * j_{ez+1}) -$$
$$- n_{1z} * n_e * j_{ez}^v + n_{1z+1} * n_e * j_{ez+1}^v - n_{1z} * n_{2z+1} * j_{12}^z - n_{1z} * n_{2z-1} * j_{21}^{z-1} + \qquad (2.7).$$
$$+ n_{2z} * n_{1z-1} * j_{21}^z + n_{2z} * n_{1z+1} * j_{21}^{z+1}$$

The similar expression is for S_{2z}. A detail analysis of reaction rates, expression for variation rate of electron temperature in non-elastic processes S_{ee} and expressions for energy transfer in elastic collisions Q_1, Q_2 and Q_e are presented in the previous report. It is significant that the variation of T_e due to yield of photorecombination radiation is already taken into account with sufficient accuracy. The terms with braking and magnetic braking radiation are added in S_{ee} by separate terms, since they did not connect with non-elastic kinetic processes.

Electron thermal conductivity is defined by the coefficient:

$$\lambda_e = \frac{(kT_e)^{5/2}}{m_e^{1/2} * Z * e^4 * \ln \Lambda}; \; 1/\text{см*с}. \qquad (2.8).$$

From the simple estimations it follows, that the characteristic distance of heat propagation by electron thermal conductivity in a time of the interaction of incoming and reflected flows ($\tau \sim 4*10^{-8}$ s) is defined by a coefficient of temperature conductivity $\chi_e = \frac{2}{3} * \frac{\lambda_e}{n_e}$ and has the value $L \cong \sqrt{\chi_e * \tau}$ comparable to CT radius. However, taking into account that the scheme itself has a differential dissipation and in our attempt to understand in more detail the features of interaction in a process of the interpenetration of incoming and reflected flows, we are restricted only by the effect of differential dissipation.

The basic requirements that we posed at development of the kinetics-temperature block are autonomy, universality and economy of calculation in time. The autonomy should allow to use the block for solving of extended problem categories, essentially independent of gas dynamics flow pattern and of the chosen grid - type of Lagrangian or Euler. In this case the particle velocities and densities should be by input parameters for calculation (α_{iz}, $T_{e,i}$) at a future time layer. The block universality should provide a possibilty of calculation (α_{iz}, $T_{e,i}$) essentially in any wide, but reasonable range of the variation of initial data: $n \leq 10^{22}$ cm^{-3}, T=

$0.025 \div 100$ кeV. Since the implicit differential schemes are on the base of calculation algorithm (α_{iz}, $T_{e,i}$), then the special attention is focused on the convergence of iteration process - its rapidity and economy in time.

Since the equation for $\alpha_{1z}=n_{1z}/n_1$ and $\alpha_{2z}=n_{2z}/n_2$ are linear, in the general case of the no quasineutrality the equation for $\alpha=n_e/(n_1+n_2)$ is calculated separately and the iteration ⎕$_{2z}$ α is created that is rapidly converged under n_1, $n_2 \leq$ $5.*10^{19}$ cm^{-3}. In our problem, as shown in numerical experiment, some deviation from the quasineutrality is observed only near sharp fronts. In general the quasineutral approximation is applicable and the iteration are carried out with the relation:

$$\alpha = \sum_z Z * \alpha_{1z} + \sum_z Z * \alpha_{2z} \qquad (2.9).$$

However, the iterations are not satisfied to universality criteria, since at $n > 5.*10^{19} \div 10^{20}$ cm^{-3} their convergence slows down sharply at $T \leq 1$ eV. Therefore the special iteration processes was developed, which in the field of single ionization at high particle density up to 10^{22} cm^{-3} produced the rapid convergence. So, the kinetic calculation block (α_{1z}, α_{2z}, α) in the last version is satisfied to all requirements outlined above.

The similar requirements are on the base of the production of the block of temperatures T_e, T_1, T_2 calculation. We proposed an idea of decomposition of temperature equation on physical processes. Through introduction of so called temperatures y_1, y_2, y_e:

$$y_1=T_1/T_{1g}, \qquad y_2=T_2/T_{2g}, \qquad y_e=T_e/T_{eg} \qquad (2.10),$$

in temperature equations we can decompose the terms responsible for adiabatic expansion ($n_i * T_i * div\vec{V}_i$) from ones corresponding to non-elastic and elastic collisions (Q_1,Q_2,Q_e,S_{ee}). Substitution of (2.10) in (2.4-2.6) gives for adiabatic temperatures T_{1g},T_{2g} the equations:

$$\frac{3.}{2.} * \frac{dT_{ig}}{dt} + T_{ig} * div\vec{V}_i = 0., \text{ где i=1,2,} \qquad (2.11),$$

that in combination with continuity equations:

$$\frac{\partial n_i}{\partial t} + div(n_i * \vec{V}_i) = 0., \text{ где } n_i = \sum_z n_{iz} \qquad (2.12),$$

have the solutions $\dfrac{T_{ig}^{3/2}}{n_i} = const$. In doing so, for kinetic temperatures y_i the equations are taken without divergent terms:

$$\frac{dy_i}{dt} = \frac{2}{3} * \frac{Q_i}{n_i * T_{ig}} \text{, где } i=1,2 \qquad (2.13).$$

The continuity equation for electrons (2.3) has a non-zero right hand, therefore substituting (2.10) in (2.6) we obtain the equation:

$$\frac{3}{2} * n_e * T_{eg} * \frac{dy_e}{dt} + n_e * T_e * \left(\frac{3}{2} * \frac{1}{T_{eg}} * \frac{dT_{eg}}{dt} - \frac{1}{n_e} * \frac{dn_e}{dt} \right) + T_e * S_e = Q_e + S_{ee} \qquad (2.14).$$

Equating the expression in parenthesis to zero, we get the decomposed equation system for calculation of electron temperature:

$$\begin{cases} \dfrac{3}{2} * n_e * T_{eg} * \dfrac{dy_e}{dt} = Q_e - T_e * S_e + S_{ee} \\ \dfrac{T_{eg}^{3/2}}{n_e} = const \end{cases} \qquad (2.15).$$

The described idea of decomposition is convenient to the Lagrangian grids, since it allows one to transform the equation system in partial derivatives to a system of regular differential equations. However, with the Euler grid, using the "method of big particles" as it adequately describes physics of gas dynamics processes , the Lagrangian type of calculation corresponds to the described decomposition method. Without introduction of decomposition method the terms ($n_i * T_i * div\vec{V}_i$) introduce additional approximation errors, since the used form of temperature equations (2.4)-(2.6) is not a divergant-conservative.

It should be emphasized that main calculation difficulties were connected with the terms Q_1, Q_2, Q_e, S_{ee} in temperature equations. This needed the development of implicit differential scheme and organization of special iteration process, this work is completely performed in the frame of given contract. In calculations the main result was achieved: rapid convergence of iteration process at reasonable accuracy ($\sim 1\%$).

3. Momentum and Energy Transfer Rate

For a wide range of plasma current conditions a local Maxwellian particle velocities distribution is applicable in terms of their directed motion velocities. As a result of the detail analysis we obtained the rather complete expressions for $\vec{R}_{12}$ and

Q some of which were already used to solve the problems of clot collisions. With these expressions for further studies, we show them here in the rather complete form:

$$\vec{R}_1 = \vec{R}_{1i} + \vec{R}_{10} + \vec{R}_{1e} \tag{3.1}$$

First term corresponds to collisions with ions, second - with neutrals, and third - with electrons:

$$\vec{R}_{1i} = \frac{4\pi e^4 * \overline{Z}_1^2 * \overline{Z}_2^2}{\mu * W^3} * n_1 * n_{2i} * (\vec{V}_2 - \vec{V}_1) * L * F_i(x)$$

$$\vec{R}_{10} = \frac{\mu \sigma_{12} a}{\sqrt{\pi}} * n_1 * n_{20} * (\vec{V}_2 - \vec{V}_1) * F_0(x)$$

$$(3.2),$$

$$\vec{R}_{1e} = \frac{4\pi e^4 * \overline{Z}_1^2 * L}{m_e * W_{1e}^3} * n_{1i} * n_e * (\vec{V}_e - \vec{V}_1) * F_e(x_{1e})$$

$$(3.3).$$

The expression for $\vec{R}_2$ has a similar form. For electrons we get:

$$\vec{R}_e = -\frac{4\pi e^4 L}{m_e} * n_e * [\frac{\overline{Z}_1^2 * n_{1i}}{W_{1e}^3} * (\vec{V}_e - \vec{V}_1) * F_e(x_{1e}) + \frac{\overline{Z}_2^2 * n_{2i}}{W_{2e}^3} * (\vec{V}_e - \vec{V}_2) * F_e(x_{2e})]$$

$$(3.4).$$

Here:

$$\overline{Z}_1 = \frac{\sum_z n_{1z} * Z}{n_1}; \; \overline{Z}_2 = \frac{\sum_z n_{2z} * Z}{n_2}; \; \mu = m_1 * m_2 / (m_1 + m_2);$$

$$n_{1i} = \sum_{z=1}^{zm} n_{1z} = n_1 * \sum_{z=1}^{zm} \overline{\alpha}_z;$$

$$n_{2i} = \sum_{z=1}^{zm} n_{2z} = n_2 * \sum_{z=1}^{zm} \overline{\alpha}_z; \; n_{10} = \overline{\overline{\alpha}}_0 * n_1; \; n_{20} = \overline{\overline{\alpha}}_0 * n_2;$$

$$W = |\vec{V}_2 - \vec{V}_1| = \sqrt{(V_{2z} - V_{1z})^2 + (V_{2r} - V_{1r})^2}$$

$$W_{1e} = |\vec{V}_e - \vec{V}_1|; \; W_{2e} = |\vec{V}_e - \vec{V}_2|; \; x = \frac{W}{\sqrt{2kT_1/m_1 + 2kT_2/m_2}}; \; a = \sqrt{2kT_1/m_1 + 2kT_2/m_2};$$

$$x_{1e} = W_{1e}/\sqrt{2kT_e/m_e}; \; x_{2e} = W_{2e}/\sqrt{2kT_e/m_e}$$

$$(3.5).$$

The σ_{12} is the ion-neutral collisional cross section. For energy transfer rate we get: $Q_1 = Q_{1i} + Q_{1o} + Q_{1e}$, where:

$$Q_{1i} = \frac{4\pi e^4 Z_1^2 Z_2^2 L}{\mu * W} n_{1i} n_{2i} * \{\frac{\mu(T_2 - T_1)}{m_1 T_2 + m_2 T_1} * \Phi(x) +$$

$$\frac{m_2 T_1 \vec{V_1} + m_1 T_2 \vec{V_2}}{m_2 T_1 + m_1 T_2} \frac{\vec{W}}{W^2} * [\Phi(x) - \frac{2x}{\sqrt{\pi}} \exp(-x^2)]\}$$

$$Q_{1o} = \frac{\mu \sigma_{12} a^2}{\sqrt{\pi}} * n_1 * n_{20} * \{\frac{\mu(T_2 - T_1)}{m_1 T_2 + m_2 T_1} * \Psi(x) + \frac{m_2 T_1 \vec{V_1} + m_1 T_2 \vec{V_2}}{m_2 T_1 + m_1 T_2} * \frac{\vec{W}}{a^2} * F_0(x)\}$$

$$Q_{1e} = \frac{4\pi e^4 Z_1^2}{m_e * W_{1e}} * n_{1i} * n_e * \{\frac{m_e (T_e - T_1)}{m_1} * \Phi(x_{1e}) + \frac{\vec{V_e} * \vec{W_{e1}}}{W_{e1}^2} * [\Phi(x_{1e}) - \frac{2x_{1e}}{\sqrt{\pi}} * \exp(-x_{1e}^2)]\}$$

(3.6).

Here: $\vec{W} = \vec{V_2} - \vec{V_1}$; $\vec{W_{e1}} = \vec{V_e} - \vec{V_1}$; $W = |\vec{W}|$; $W_{1e} = |\vec{W_{1e}}|$.

The expression for Q_2 has a similar form. For Q_e we find (with $m_e << m_i$):

$$Q_e = -\frac{4\pi e^4 n_e L}{m_e} * \sum_{k=1}^{2} \frac{\bar{Z_k} * n_{ki}}{W_{ke}} * \{\frac{m_e}{m_k} * \frac{T_e - T_k}{T_e} * \Phi(x_{ke})$$

$$+ \frac{\vec{V_e} * \vec{W_{ek}}}{W_{ek}^2} * [\Phi(x_{ke}) - \frac{2x_{ke}}{\sqrt{\pi}} * \exp(-x_{ke}^2)]\}$$

(3.7).

Here the summation is over ion kind k=1,2. The dimensionless function arguments in right parts and their asymptotic forms look like:

$$\Phi(x) = \frac{2}{\sqrt{\pi}} * \int_0^x \exp(-t^2)\,dt = \begin{cases} \frac{2}{\sqrt{\pi}} * (x - x^3/3 + \dots); & x \to 0 \\ 1 - \frac{\exp(-x^2)}{\sqrt{\pi} * x} + \dots; & x \to \infty \end{cases}$$

$$F_i(x) = F_e(x) = \Phi(x) - \frac{2x}{\sqrt{\pi}} * \exp(-x^2) = \begin{cases} \frac{4}{\sqrt{\pi}} * (x^3/3 - x^5/5 + \dots); & x \to 0 \\ 1 - x * \exp(-x^2)/\sqrt{\pi} + \dots; & x \to \infty \end{cases}$$

$$F_0(x) = \sqrt{\pi} * x * (1 - \frac{1}{4x^4} + \frac{1}{x^2}) * \Phi(x) + (1 + \frac{1}{2x^2}) * \exp(-x^2) = \begin{cases} 8/3 + 8x^2/15; & x \to 0 \\ \sqrt{\pi} * x; & x \to \infty \end{cases}$$

$$\Psi(x) = \sqrt{\pi} * (x^3 + 3x + \frac{3x}{4}) * \Phi(x) + (x^2 + 5/2) * \exp(-x^2) = \begin{cases} 4 + 9 * x^2; & x \to 0 \\ \sqrt{\pi} * x^3; & x \to \infty \end{cases}$$

(3.8).

The analysis of cross-sections and rate coefficients is presented in the Item 2 of the report.

The system of the dimensionless kinetic equations looks like:

$$\frac{d\overline{\alpha}_0}{dt} = \overline{A}_{00}\overline{\alpha}_0 + \overline{A}_{01}\overline{\alpha}_1;$$

$$\frac{d\overline{\alpha}_1}{dt} = \overline{A}_{10}\overline{\alpha}_0 + \overline{A}_{11}\overline{\alpha}_1 + \overline{A}_{12}\overline{\alpha}_2;$$

....

....

$$\frac{d\overline{\alpha}_m}{dt} = \overline{A}_{m,m-1}\overline{\alpha}_{m-1} + \overline{A}_{m,m}\overline{\alpha}_m$$

(3.9).

It is a similar system for $\overline{\overline{\alpha}}_z$. The initial structure was determined on the quasibalance model. The values of coefficients $\overline{A}_{ij}$, $\overline{\overline{A}}_{ij}$ (one line corresponds to "1", two line correspond to "2") are determined by overcharging rate and electron kinetics. Then calculations from the kinetic block determined the ionization degree and average charges:

$$\alpha_e = \frac{n_1}{n} * \sum_1^m Z\overline{\alpha}_z + \frac{n_2}{n} * \sum_1^m Z\overline{\overline{\alpha}}_z = \frac{n_1 Z_1 + n_2 Z_2}{n};$$

$$n = n_1 + n_2; Z_1 = \sum_1^m Z * \overline{\alpha}_z; Z_2 = \sum_1^m Z\overline{\overline{\alpha}}_z$$

During the computation the conditions $\sum_1^m \overline{\alpha}_i = 1$; $\sum_1^m \overline{\overline{\alpha}}_i = 1$ are verified; the

error did not exceed 0.1%. The kinetic block for calculations of ion level populations is a similar kind, determining line spectra of plasma radiation.

4. Calculation of Linear Radiation Method

the density n_{izk} of the ion component of type i (i=1,2) and charge of Z that is excited to the electron state level k is determined by the equation:

$$\frac{\partial n_{izk}}{\partial t} + div(n_{izk} * \vec{U}_i) = S_{izk}$$

(4.1).

Here S_{izk} is the rate of the density n_{izk} change in inelastic processes:

$$S_{izk} = n_e * \left(\sum_{m \neq k} n_{izm} * j_{z,km} - n_{izk} * \sum_{m \neq k} j_{z,km}\right) + (n_e^2 * n_{i,z+1} * j_{e,z+1,k} - n_e * n_{izk} * j_{z,ke}) +$$

$$\cdot + n_e * n_{i,z+1} * j_{e,z+1,k}^v + \sum_{m>k} A_{iz,mk} * n_{izm} - n_{izk} * \sum_{m<k} A_{iz,km}$$

(4.2).

The first term in brackets corresponds to transitions between excited states as a result of electron collisions; the second term corresponds to a capture of free electron by ion (Z+1) to the level k as a result of triple collisions and the reverse process of ionization by electrons; the third term corresponds to the process of photo- and die-electron recombination to the level k of ion (Z+1); last two terms describe the change of n_{izk} as a result of spontaneous transitions between electron state levels. The estimations show that for transitions between excited states the plasma is optically transparent, while for transitions to the basic sate it is necessary to take into account the radiation reabsorption. The population of lower excited state has an especially strong effect on populations of excited states. The transition from this state (2→1) corresponds to so-called resonance radiation. Usually, to take into account a self-absorption of the resonance radiation, the approximation of Biberman-Holstein [2,3] is used by the inputting of photon escape probability Θ_z from a plasma volume.

We obtained the sufficiently general expressions for Θ by the example of expanding plasma volume, when the plasma layers moved relative to each other, and sufficiently convenient for calculations the approximation function is given:

$$\Theta = \frac{\Delta}{\Delta + \frac{3}{7}*\tau} + \frac{3/7*\tau}{\left(\Delta + \frac{3}{7}*\tau\right)*\left(\sqrt{3} + \sqrt{\tau*\left(1 - \frac{r}{R}\right)}\right)}$$

(4.3).

Here $\Delta = \frac{2*\omega_0*U_0}{c*\Delta\omega}$ is the ratio of the Doppler shift to the line half-width; ω_0 is the frequency at the line center; U_0 is the relative speed of plasma flows; c is the light speed; $\Delta\omega$ is the effective line width; R is the effective radius of plasma volume V ($R \sim \sqrt[3]{\frac{3*V}{4*\pi}}$); r is the effective distance from plasma center up to point of radiation. In particular, from (3) it may be concluded that plasma motion begins to effect on Θ at $\Delta > \sqrt{\tau}$. At $\tau = 0$ we have $\Theta = 1$ and at r=R, that is on the plasma boundary (at $\Delta \ll \tau \gg 1$), we can obtain $\Theta = \frac{1}{\sqrt{3}}$. So, slightly more than the half of radiation freely yields the plasma clot region. At $\Delta \to 0$ (that is at $U_0 \to 0$) the expression (3) transforms to known expression for plasma at rest, but takes into account the distance to plasma volume boundary more precisely. The expression for τ corresponding to transition k→1 of ion Z takes the form:

$$\tau = \frac{\lambda_{z,k1}^2}{4} * \frac{A_{zk1}}{\Delta\omega_z} * n_z * R$$

(4.4).

where $\lambda_{z,k1} = 1.24 * 10^{-4} / E_{zk}(eV)$, cm is the wavelength of transition k→1 for ion Z; E_{zk} is the energy of level k relative the basic state.

The expressions for probabilities of spontaneous and collisional transitions were presented in the Item 4 of the report.

All plasma optical characteristics and first the intensity of its linear radiation may be determined by solving a system of linear equations relative to α_{izk} for each Z:

$$\alpha_{izk} * \left(\sum_{\substack{m=1 \\ m \neq k}}^{10} j_{z,km} + j_{z,ke} + \frac{1}{\alpha * n} * \sum_{m<k} A_{zz,km} * \Theta_{km} \right) -$$

$$- \sum_{\substack{m=1 \\ m \neq k}}^{10} \alpha_{izm} * \left(j_{z,mk} + \frac{1}{\alpha * n} * A_{iz,mk}(m > k) \right) =$$

$$= \alpha_{i,z+1} * (\alpha * n * j_{e,z+1,k} + j_{e,z+1,k}^{v})$$

(4.5).

The power radiation in the given line is defined by expression:

$$\varepsilon_{izkm} = A_{z,km} * E_{z,km} * n_{izk}, \text{ eV/cm3*s.}$$

In the region of the existence of incoming and reflected flows:

$$\varepsilon_{zkm} = A_{z,km} * E_{z,km} * (n_{1zk} + n_{2zk}) = A_{z,km} * E_{z,km} * (\alpha_{1zk} * n_1 + \alpha_{2zk} * n_2) =$$

$$= A_{z,km} * E_{z,km} * \alpha_{zk} * (n_1 + n_2) = A_{z,km} * E_{z,km} * \alpha_{zk} * n, \text{ eV/cm3*s.}$$

In these transformations it is supposed that $\alpha_{1zk} \cong \alpha_{2zk} = \alpha_{zk}$, since they are determined primarily by electron temperature and density. The slight difference in α_{1zk} and α_{2zk} obtained in calculations, plays no important role in the analysis of plasma linear radiation.

5. Statement of Dynamic and Electromagnetic Problem
5.1. Motion and temperature equations

It is supposed that ions of all charges of incoming component have velocity $\vec{V}_1$, ions of all charges of reflected component - velocity $\vec{V}_2$, electrons - velocity $\vec{V}_e$. Then for ions of charge Z of incoming component the motion equation takes the form:

$$m_1 * n_{Z_1} * \left(\frac{\partial \vec{V}_1}{\partial t} + (\vec{V}_1 \nabla)\vec{V}_1 \right) = -\nabla P_{Z_1} + n_{Z_1} * Z_1 * e * \left(\vec{E} + \frac{1}{c} * \vec{V}_1 \times \vec{B} \right) + \vec{R}_{Z_1}$$

(5.1).

where $\vec{R}_{Z_1} = \sum_{Z_2} \vec{R}_{Z_1,Z_2} + \vec{R}_{Z_1,e}$ is the friction force of ions Z_1 with all ions of the second component and electrons. This value is proportional to $\vec{R}_{Z_1,Z_2} \sim Z_1^2 * n_{1Z} * Z_2^2 * n_{2Z}$. Since all ions with Z_1 have velocity $\vec{V}_1$, we can obtain the sum in friction force by summing equations (5.1) over all Z_1:

$$\left(\sum_{Z_1} Z_1^2 * n_{Z_1}\right) * \left(\sum_{Z_2} Z_2^2 * n_{Z_2}\right) = n_1 * n_2 * \left(\sum Z_1^2 * \overline{\alpha}_Z\right) * \left(\sum Z_2^2 * \overline{\overline{\alpha}}_Z\right), \qquad \text{where} \qquad \overline{\alpha}_Z = \frac{n_{Z_1}}{n_1};$$

$\overline{\overline{\alpha}}_Z = \frac{n_{Z_2}}{n_2}$, and in the electrodynamic term you can find the linear sum

$\sum_{Z_1} Z_1 * n_{Z_1} = n_1 * \sum Z_1 * \overline{\alpha}_Z$. The calculations showed that the difference under root-

men-square and linear averaging is negligibly small:

T,eV	5	10	20	35
$\overline{Z}$	1.99	3.90	6.75	7.87
$\sqrt{\overline{Z^2}}$	2.015	3.97	6.79	7.86

Because of this the $\overline{Z}$ is used in all calculations.

In such a manner the dynamic equations take the form:

$$m_i * n_i * \frac{d\vec{V}_i}{dt} = -\nabla P_i + e * \overline{Z}_i * n_i * \left(\vec{E} + \frac{1}{c} * \vec{V}_i \times \vec{B}\right) + \vec{R}_i$$

(5.2)

$$m_e * n_e * \frac{d\vec{V}_e}{dt} = -\nabla P_e - e * n_e * \left(\vec{E} + \frac{1}{c} * \vec{V}_e \times \vec{B}\right) + \vec{R}_e$$

(5.3).

Here i=1,2. We have $m_1=m_2=m$; $P_i=n_i*T_i$; $P_e=n_e*T_e$ for incoming and reflected flows. The full expressions for $\vec{R}_i, \vec{R}_e$ and also the equations for T_1, T_2, T_e and their terms are given discussed above.

5.2. Electromagnetic field equations

The complete equation system describing the dynamics of three-fluid plasma may be obtained by addition of Maxwell equation system to dynamics, temperature and continuity equations:

$$\frac{\partial \vec{B}}{\partial t} = -c * rot\vec{E}$$

(5.4)

$$\frac{\partial \vec{E}}{\partial t} = -4 * \pi * \vec{j} + c * rot\vec{B}$$

(5.5)

$$div\vec{E} = 4 * \pi * \rho_e$$

(5.6)

$$div\vec{B} = 0.$$

(5.7),

where the densities of electric current $\vec{j}$ and charge ρ_e are defined by plasma motion

$$\vec{j} = \vec{V}_1 * e * \sum n_{Z_1} * Z_1 + \vec{V}_2 * e * \sum n_{Z_2} * Z_2 - e * n_e * \vec{V}_e =$$
$$= e * n_1 * \overline{Z}_1 * \vec{V}_1 + e * n_2 * \overline{Z}_2 * \vec{V}_2 - e * n_e * \vec{V}_e$$

(5.8)

$$\rho_e = e * n_1 * \overline{Z}_1 + e * n_2 * \overline{Z}_2 - e * n_e$$

(5.9).

When large-scale low-frequency plasma motions are considered rather than internal plasma vibrations, the electron generation play no essential role in formation of $(\vec{E}, \vec{B})$ fields, since the plasma, by any way, tends to be a quasineutral. Therefore in typical plasmodynamics problems the field $\vec{E}$ is determined from motion equation for electrons, and then the charge density ρ_e (if it is necessary to estimate ρ_e for sharp fronts) is defined from the Poison equation (5.6). By doing so, the quasineutrality condition may be used in dynamics and kinetics equations with high accuracy while $div\vec{E} \neq 0..$ This is so-called plasma approximation that we use in the given problem.

In the region of intensive interaction where $\dfrac{\left|\vec{V}_i - \vec{V}_e\right|}{\sqrt{\dfrac{2kT_e}{m_e}}} \leq 1.$, we can mark the main

dependence of velocities in the expression for $\vec{R}_e$

$$\vec{R}_e = -m_e * n_e * \left(\frac{\vec{V}_e - \vec{V}_1}{\tau_{e1}} + \frac{\vec{V}_e - \vec{V}_2}{\tau_{e2}} \right)$$

(5.10),

where τ_{e1}, τ_{e2} were taken from the general expression for $\vec{R}_e$ obtained and given above. Such presentation is required only to obtain the complete equation system for field; the strict expression for $\vec{R}_e$ was used in the dynamics equation. In such a manner, we can obtain from (5.3)

$$\vec{E} = -\frac{1}{c}*[\vec{V_e} \times \vec{B}] - \frac{\nabla P_e}{e*n_e} - \frac{m_e}{e}*\left(\frac{\vec{V_e}-\vec{V_1}}{\tau_{e1}} + \frac{\vec{V_e}-\vec{V_2}}{\tau_{e2}}\right)$$

(5.11).

Substituting $\vec{V_e}$ from (5.8) in (5.11) we obtain:

$$\vec{E} = -\frac{1}{c}*[\vec{V} \times \vec{B}] + \frac{1}{e*c*n_e}*[\vec{j} \times \vec{B}] - \frac{\nabla P_e}{e*n_e} + \frac{\vec{j}}{\sigma} +$$

$$+ e*\left(\frac{\overline{Z_2}*n_2}{\sigma_1} - \frac{\overline{Z_1}*n_1}{\sigma_2}\right)*\left(\vec{V_1} - \vec{V_2}\right)$$

(5.12).

where the last term may be simplified as a result of using of the quasineutrality condition which, as seen from the structure of this term itself, play no fundamental role. Here $\vec{V} = \left(\overline{Z_1}*n_1*\vec{V_1} + \overline{Z_2}*n_2*\vec{V_2}\right)/n_e$ is the mean-charge ion velocity; $\sigma_1 = e^2*n_e*\tau_{e1}/m_e;$ $\sigma_2 = e^2*n_e*\tau_{e2}/m_e$ are the partial conductivity, and $\sigma = \sigma_1*\sigma_2/(\sigma_1 + \sigma_2)$ is the total plasma conductivity. Expression (5.12) is essentially the Ohm's law taking into account the Haul effect, in which the last term is characteristic for two ion flows.

Neglecting of displacement current in (5.5), since $\left|\vec{V_1}\right|, \left|\vec{V_2}\right|, \left|\vec{V_e}\right| \ll c$, we obtain

$$\vec{j} = \frac{c}{4\pi}*rot\vec{B}$$

(5.13).

Substituting in (5.12), taking into account (5.4), we obtain the system of two equations for determination of fields $(\vec{E}, \vec{B})$:

$$\vec{E} = -\frac{1}{c}*[\vec{V} \times \vec{B}] + \frac{1}{4\pi e n_e}*[rot\vec{B} \times \vec{B}] + \frac{c}{4\pi\sigma}*rot\vec{B} -$$

$$- \frac{\nabla P_e}{en_e} + e*\left(\frac{\overline{Z_2}*n_2}{\sigma_1} - \frac{\overline{Z_1}*n_1}{\sigma_2}\right)*\left(\vec{V_1} - \vec{V_2}\right)$$

(5.14);

$$\frac{\partial \vec{B}}{\partial t} = -c*rot\vec{E}$$

(5.15).

When substituting the expression for $\vec{E}$ from (5.14) in (5.15), we can obtain equation for $\vec{B}$ in diffusion form, with two last terms in (5.14) that will be responsible for magnetic field generation.

A full numerical problem solution on determination of field $\vec{B}$ from equation (5.15) on dynamic plasma characteristic represents problem for itself and demands the development of special two-dimensional algorithm. In the present time the basics for such algorithm were developed with decomposition method on physical processes.

In frame of the present work it is planned, in accordance with contract contents, to carry out the approximate field calculation with a number of simplifications that are typical for given problem.

Since the thermalisation of directed electron energy is much faster than that of ions $(\tau_{ee} \cong \tau_{ii} * \sqrt{m/M})$, electron gas behave as continuous medium behind the reflected wave in the absence of friction forces over ions and have $\vec{V}_e = 0$. On the other hand, if the friction force between electrons and ions is dominant in equation (5.13), and the force between ions is not too high, then $n_1 \approx n_2; |\vec{V}_1| = |\vec{V}_2|; \dfrac{\partial P_e}{\partial x} \approx 0; \tau_{e1} \approx \tau_{e2}$, and

from equation $-\dfrac{m_e * n_e * (V_e - V_1)}{\tau_{e1}} - \dfrac{m_e * n_e * (V_e + V_2)}{\tau_{e2}} \approx 0$ we obtain $V_e \approx V_1 - V_2 \approx 0$.

Thus the friction over ions «1» and «2» acts in opposite directions and again V_e is close to zero. It immediately follows that electric field due to low velocities values V_e, plays no important role in the region of interpenetrating of incoming and reflected flows. Magnetic field can not significantly effect on plasma parameters due to short interaction time. By doing so, in the first approximation the field problem may be considered as not self-consistent, that is, to take no account the reverse effect of field on plasma. Then from kinetics and dynamics equations (5.2), (5.3) (without considering the fields) we obtain current value (5.8) and from equation (5.13), that presents simply the Biot-Savart law, we obtain field value along zone of flows interaction. The calculations of external magnetic field, carried by such a manner, are presented in figures and in appendix and represent the upper estimation for its amplitude.

5.3. Boundary conditions

The initial moment t=0 corresponded to contact moment of incoming flows with a target. Flow characteristics at this moment of time take the form in dimensionless units:

$$\text{a) } n_1 = 1; \ 0 \le x \le a; \ 0 \le r \le R,$$

$$n_2 = 0; \ 0 < x \le a; \ 0 \le r \le R,$$

$$n_2 = 1; \ x = 0; \ 0 \le r \le R,$$

$$\text{b) } U_1 = -1; \ 0 \le x \le a; \ 0 \le r \le R,$$

$$V_1 = 0; \ 0 \le x \le a; \ 0 \le r \le R,$$

$$U_2 = 1; \ x = 0; \ 0 \le r \le R,$$

$$V_2 = 0; \ x = 0; \ 0 \le r \le R,$$

$$\text{c) } U_e = -1; \ 0 < x \le a; \ 0 \le r \le R,$$

$$V_e = 0; \ 0 < x \le a; \ 0 \le r \le R,$$

$$\text{d) } T_1 = 20 \text{ eV}, \ 0 \le x \le a; \ 0 \le r \le R,$$

$$T_2 = 20 \text{ eV}, \ x = 0; \ 0 \le r \le R,$$

$$T_e = 20 \text{ eV}, \ 0 \le x \le a; \ 0 \le r \le R.$$

In all free boundaries $P_1 = P_2 = P_e = 0$.

In the target surface (x=0):

$$U_2(x = 0) = -U_1(x = 0),$$

$$U_e(x = 0) = V_e(x = 0) = 0,$$

$$V_2(x = 0) = V_1(x = 0).$$

By this means, in frame of contract all physical processes connected with dynamics and interaction with a target the plasma clot oriented to facility "Marauder" were fully analyzed. The complete equation system was formulated and the two-dimensional numerical algorithm was developed which allows one to determine all basic characteristics of the interaction zone of plasma clot with target: charge composition, ionization degree, temperatures T_1, T_2, T_e, velocities $\vec{V}_1, \vec{V}_2, \vec{V}_e$ and concentrations n_1, n_2, n_e of plasma flows, to calculate continuum and linear plasma radiation, to estimate electromagnetic fields.

The program text, user's guide and examples of calculations are given in the report appendix.

6. Conclusions

1. The given work gives sufficiently full presentation that is going and may be achieved for high temperatures under plasma conditions using the scheme:

```
┌─────────────────────────────────────────┐
│   Electromagnetic generator energy        │
└─────────────────────────────────────────┘
                   │
┌─────────────────────────────────────────┐
│      Kinetic energy of plasma clot        │
└─────────────────────────────────────────┘
                   │
┌─────────────────────────────────────────┐
│        Thermal plasma energy              │
└─────────────────────────────────────────┘
```
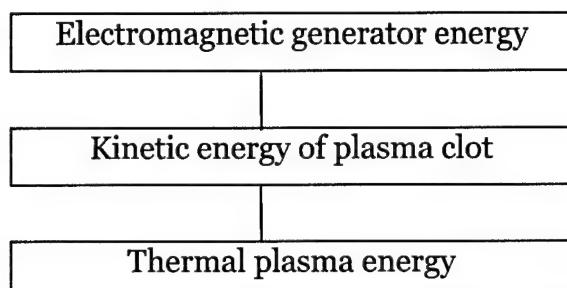
Taking into account the generator possibilities it is unlikely that the temperatures are not higher than ~10 KeV. In addition, a number of physical restrictions exists.

2. In our opinion, the most interesting is the interaction region of incoming and reflected flows as a source of x-ray radiation that is, due to its high penetration, can effect on the space behind target, change the conductivity and destroy optical-electronic elements. The given work besides all questions may solve the problem on the source of such radiation.

3. The impulse of electromagnetic field in the meter and decameter range presents also the essential applied interest. The pulse can produce the interference in electrical-technical systems operation. However, the calculation of such electromagnetic pulse is the complicated two-dimensional problem. In the given report on the base of approximate numerical solution it is shown that amplitude of magnetic component of such impulse may be up to 10^5-10^6 Gauss.

In such a manner, the electromagnetic radiation in different ranges may be of essential interest in this problem.
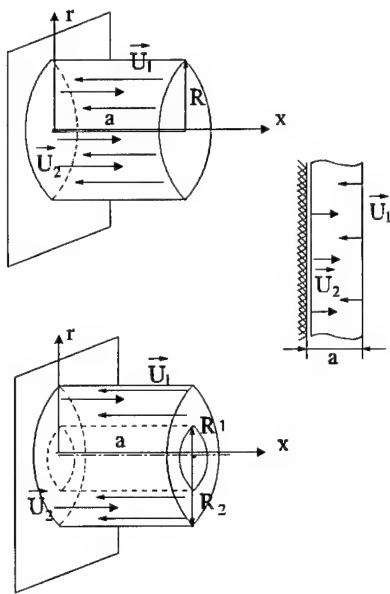
Fig.1. Spatial and energetic characteristics of plasma clots colliding with a target:
T_0=20-30 eV, U_0=10^7-10^8 cm/s, n_0=10^{16}-10^{19} cm^{-3}
a=3 cm, R=3 cm, R_1=0.25 *R, R_2=0.75*R
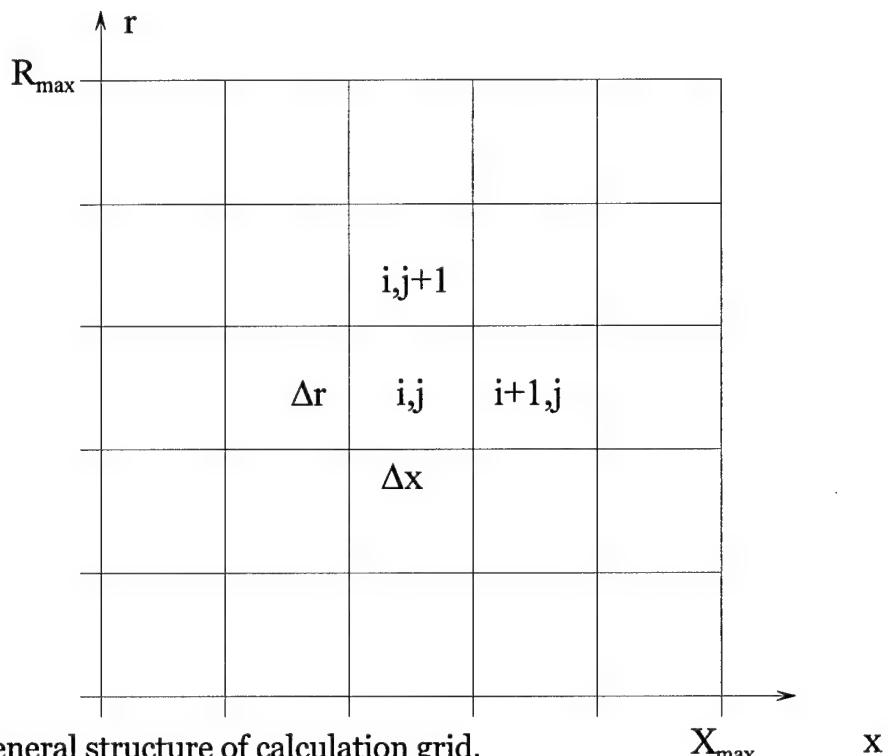
Fig.2. General structure of calculation grid.
Values calculated at time layer n:
$U_1(i,j)$, $V_1(i,j)$, $U_2(i,j)$, $V_2(i,j)$, $U_e(i,j)$, $V_e(i,j)$
$T_1(i,j)$, $T_2(i,j)$, $T_e(i,j)$, $n_1(i,j)$, $n_2(i,j)$, $n_{1zk}(i,j)$, $n_{2zk}(i,j)$, $E_{zkm}(i,j)$

GENERAL BLOCK SCHEME OF THE PROGRAM

Input of initial data:
n_x, T_0, n_0, $\vec{U}_0$, R_0
(file: OTL.PAR)

Calculation of characteristic values
of the problem

Preset the initial (t=0) and
boundary problem conditions

Preliminary calculation
of dynamic characteristic
(I - stage of «particle-in-cell method»),
taking into account the flows interaction,
calculation of charge composition
(SUBROUTINE STAR)

internal
iterations

Determination of substance flows
through boundaries of calculation cells
(II - stage «PIC»)

Final calculation of the characteristics
of plasma flows
(III - stage «PIC»)

$t^{n+1} = t^n + \Delta t$

Formation of files
for graph drawing

Calculation of populations
levels and radiation

$\vec{U}_1$, $\vec{U}_2$, $\vec{U}_e$,
T_1, T_2, T_e,
n_1, n_2, α_z, n_{1zk}, n_{2zk}, E_{zkm}
(U1.dat, T1.dat, AN1.dat *etc.*)

Fig.3

Figure captions:

Fig. 4 Spatial distribution of ion temperatures in the incoming and reflected plasma flows at different time moments (one-dimensional version $n_0 = 10^{17}$ cm^{-3}).

Fig. 5 Spatial distribution of ion velocities in the incoming and reflected plasma flows at different time moments (one-dimensional version $n_0 = 10^{17}$ cm^{-3}).

Fig. 6 Spatial distribution of ion densities in the incoming and reflected plasma flows at different time moments (a) and ionization degree (в) (one-dimensional version $n_0 = 10^{17}$ cm^{-3}).

Fig. 7 Spatial distribution of ion temperatures in the incoming and reflected plasma flows at different time moments (one-dimensional version $n_0 = 10^{18}$ cm^{-3}).

Fig. 8 Spatial distribution of ion velocities in the incoming and reflected plasma flows at different time moments (one-dimensional version $n_0 = 10^{18}$ cm^{-3}).

Fig. 9 Spatial distribution of ion densities in the incoming and reflected plasma flows at different time moments (a) and ionization degree (в) (one-dimensional version $n_0 = 10^{18}$ cm^{-3}).

Fig. 10 Spatial current density distribution at some time moments in the direction perpendicular to the target.

Fig. 11 Spatial distribution of longitudinal component of the generated magnetic field.

Fig. 12 Spatial distribution of ion temperatures in the incoming plasma flow at three successive time moments (two-dimensional calculation).

Fig. 13 Spatial distribution of electron temperatures at three successive time moments (two-dimensional calculation).

Fig. 14 Spatial distribution of ion temperatures in the reflected plasma flow at three successive time moments (two-dimensional calculation).

Fig. 15 Spatial distribution of ion densities in the incoming plasma flow at three successive time moments (two-dimensional calculation).

Fig. 16 Spatial distribution of ion densities in the reflected plasma flow at three successive time moments (two-dimensional calculation).

Fig. 17 Field of ion velocities in the reflected plasma flow at three successive time moments (two-dimensional calculation).

Fig. 18 Field of electron velocities at three successive time moments (two-dimensional calculation).

User's guide

Initial program text is in file **BUNCH.FOR** (programming language is «FORTRAN-77»). The initial data are introduced from file OTL.PAR, where ANX is the characteristic meaning of density (cm^{-3}), T100, T200, TE00 are the initial values of ion temperatures in the incoming flow, reflected flow, electrons (eV), U10, U20 are the initial velocity values (in dimensionless form), AA is the initial clot radius (cm) (R_x=AA), VX is the characteristic velocity value (cm/s).

In the program text itself: NX, NR are the number of cells in the calculation region of x and r, MSC determines the number of time steps for data output to files: *.DAT, MMC determines the number of time steps for control data output to BUNCH.LOG or on screen (1st column is the number of time steps, 2nd is the dimensionless time (t_x=R_x/V_x), 3rd is the dimensionless time step).

The data output to files *.DAT is in the form (for example):
WRITE(N,*) T is the time (s),
WRITE(N,*) NXX,NRR is the number of cells in x and r (размеры массивов переменных),
WRITE(N,*) (XX(I),I=0,NX) are the coordinates of cell boundaries on x (cm),
WRITE(N,*) (RR(J),J=0,NR) are the coordinates of cell boundaries on r (cm),
WRITE(N,*) ((T1(I,J),I=0,NX), J=0,NR) is the array ion temperature values in the incoming plasma flow.
Output characteristics (data arrays):
T1(I,J) is the ion temperature in the incoming flow, eV
T2(I,J) is the ion temperature in the reflected flow, eV
TE(I,J) is the electron temperature, eV,
U1(I,J) is the U_x component of the vector of ion velocity in the incoming flow, *10^8 cm/c,
V1(I,J) is the U_r component of the vector of ion velocity in the incoming flow, *10^8 cm/c,
U2(I,J) is the U_x component of the vector of ion velocity in the reflected flow, *10^8 cm/c,
V2(I,J) is the U_r component of the vector of ion velocity in the reflected flow, *10^8 cm/c,

UE(I,J) is the U_x component of the vector of electron velocity, $*10^8$ cm/c,

VE(I,J) is the U_r component of the vector of electron velocity, $*10^8$ cm/c,

AN1(I,J) is the ion density in the incoming flow $*(n_x=10^{17}$ cm^{-3}),

AN2(I,J) is the ion density in the reflected flow $*(n_x=10^{17}$ см$^{-3}$),

AALFS(I,J) is the ionization degree α,

LIN(I,J,IZ,M,K) is the array of radiation coefficients E_{zmk}, in cells (i,j) for ions with charge Z in transitions m→k.

To plot the isoline graphs the program **IZOLD.FOR** is used. The isoline values may be taken automatically (uniform decomposition between minimum and maximum meanings in data files), or by handle (on users's desire). To do this, the file GRAFCON1-3.DAT is used (three graphs are plotted on sheet (see the examples of twoodimensional calculations)), 7th line of this file takes the form: 1 (or 0 if automatically mode is used), 7 number of isolines, 50 100 200 300 500 750 1000 - (meanings, for example T_1, for isoline with a proper number).

To plot a field of velocities, the program **VEL.FOR** is used. During its operation first the file name should be introduced in which the meanings of 1st coordinate U_x of velocity vector are placed (for example, U1.DAT), and then the file name with meanings of 2nd coordinate U_r of vector (for example, V1.DAT). The file GRAFCON.DAT is necessary for program operation.

Following translation of files IZOLD.FOR и VEL.FOR, it is necessary to join the program library GRAFOR by the command:
$ LINK IZOLD,SYS$LIBRARY:GRAFOR/LIB.

Program translation, calculations, graph plotting were carried out on minicomputer with ALPHA processor and with operation system VAX VMS.
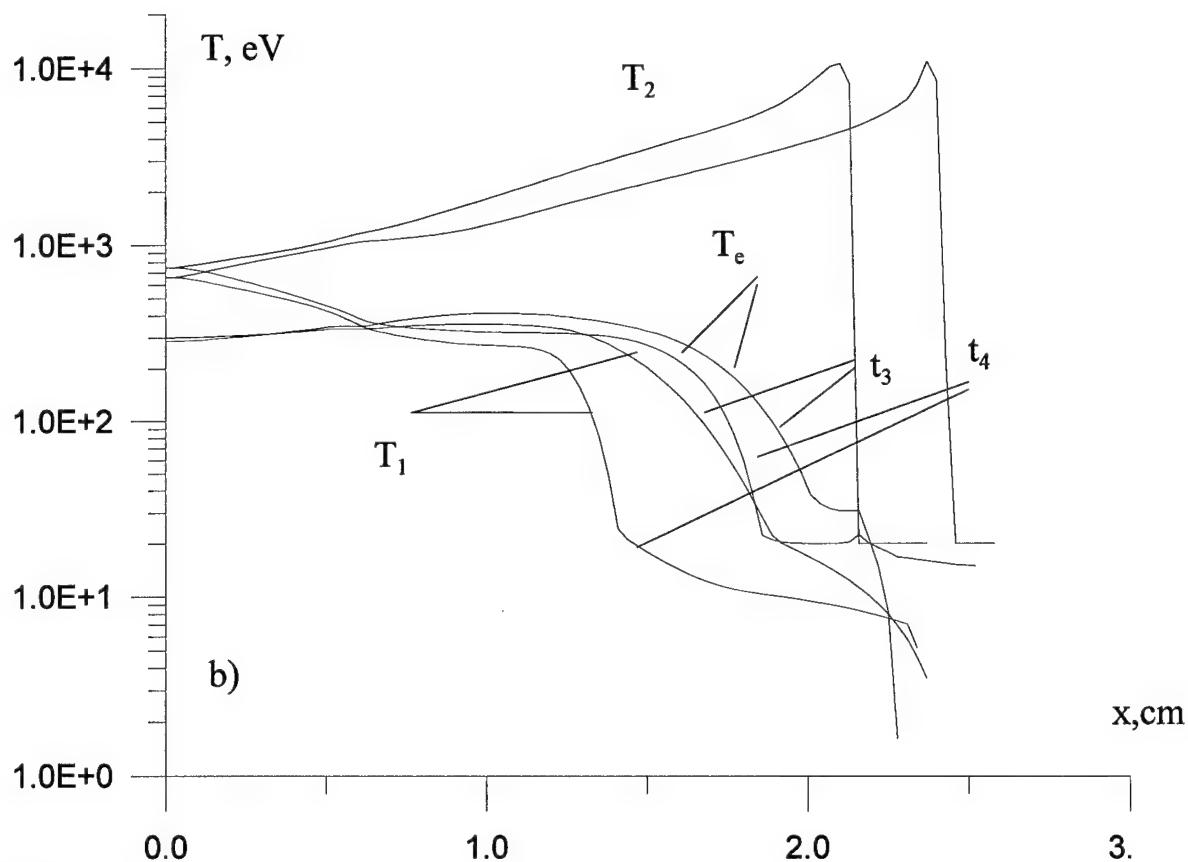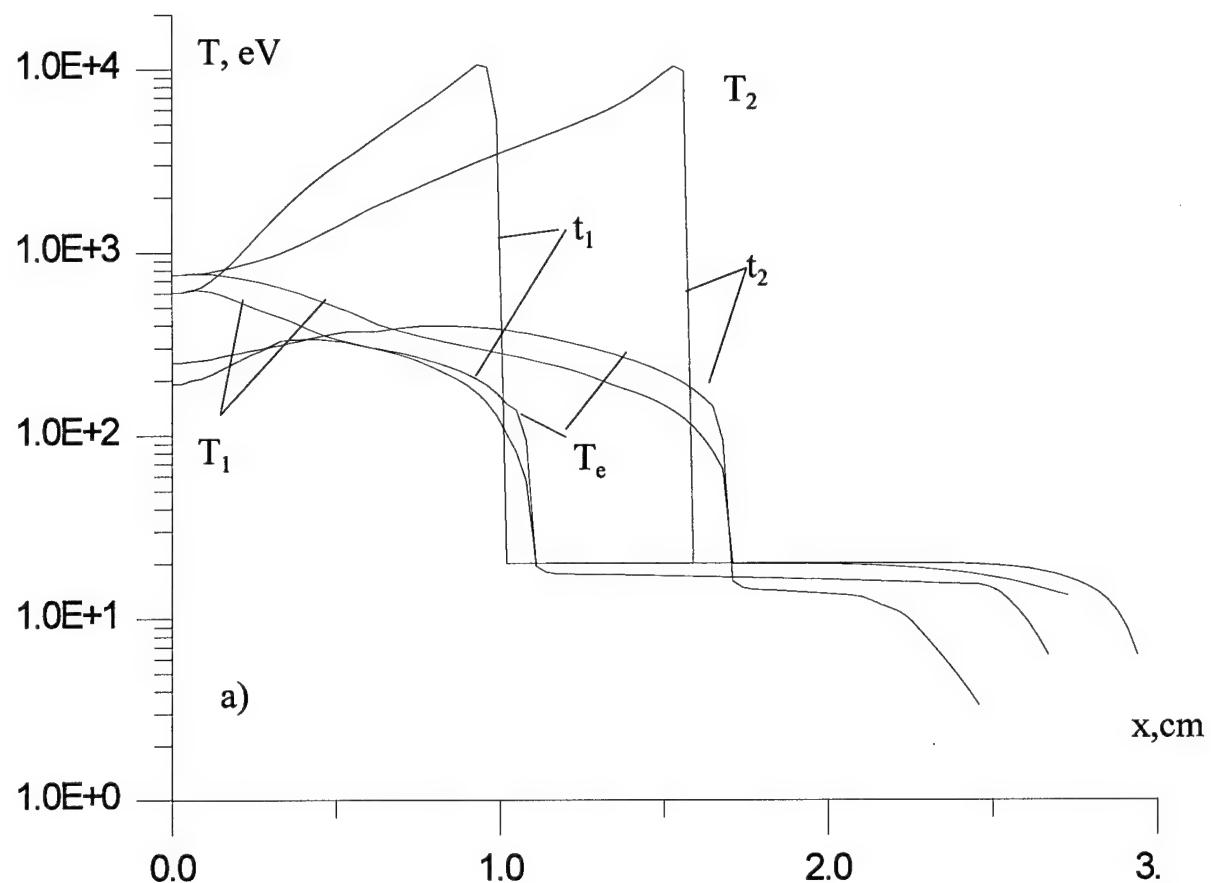
Fig. 4
$n_0=10^{17}$ cm^{-3}, $R_0=3$ cm, $V_0=10^8$ cm/s, $t_1=0.137*t_x$, $t_2=0.2621*t_x$, $t_3=0.3836*t_x$, $t_4=0.4634*t_x$, $t_x=3*10^{-8}$ s
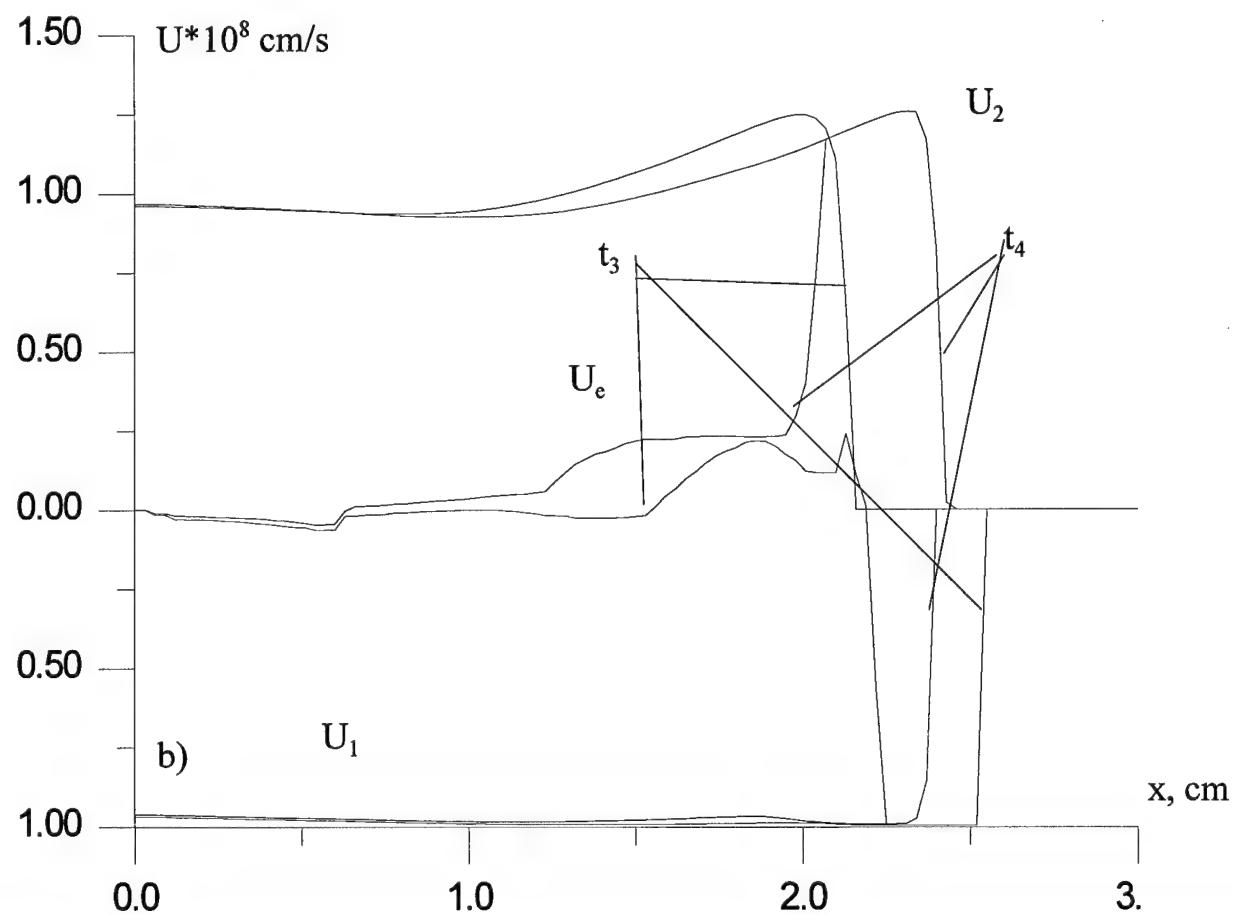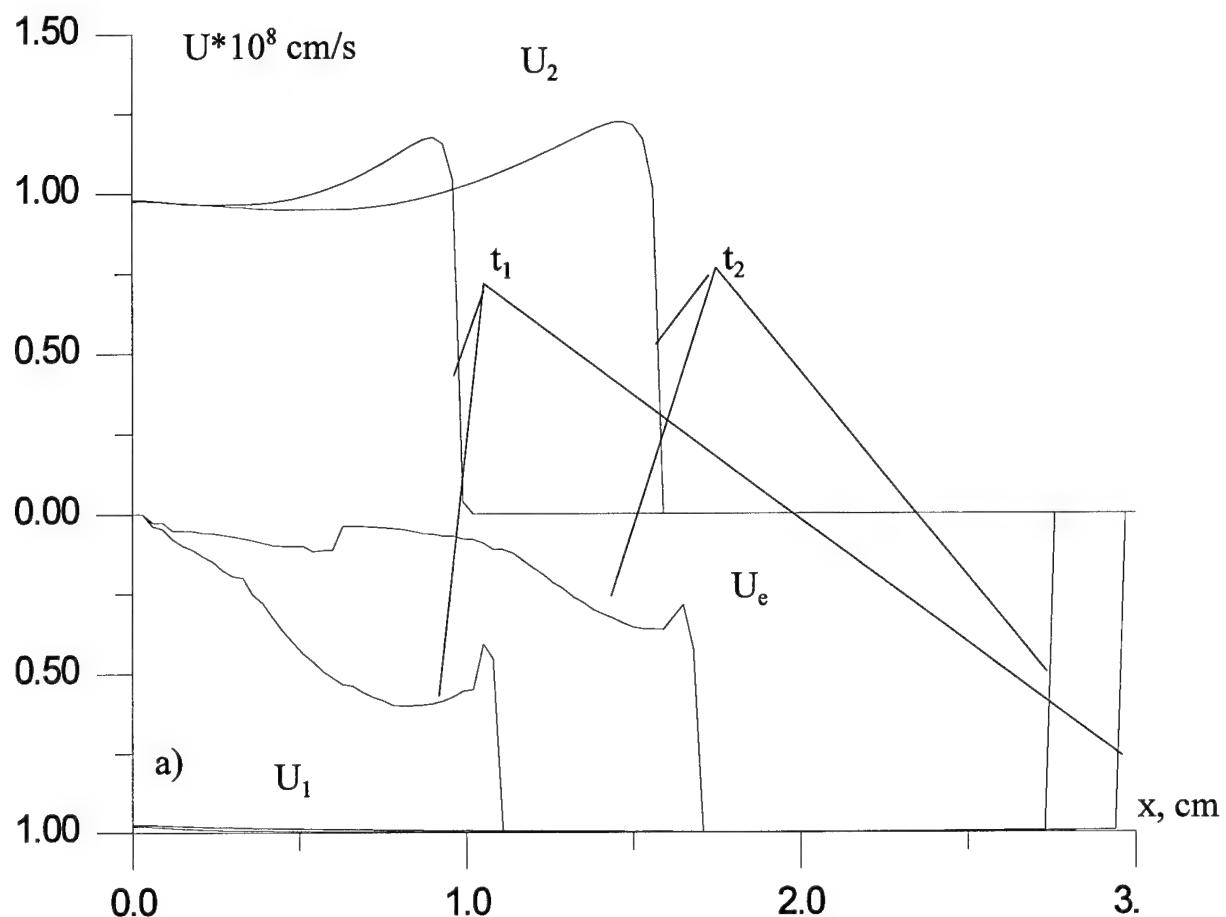
Fig. 5
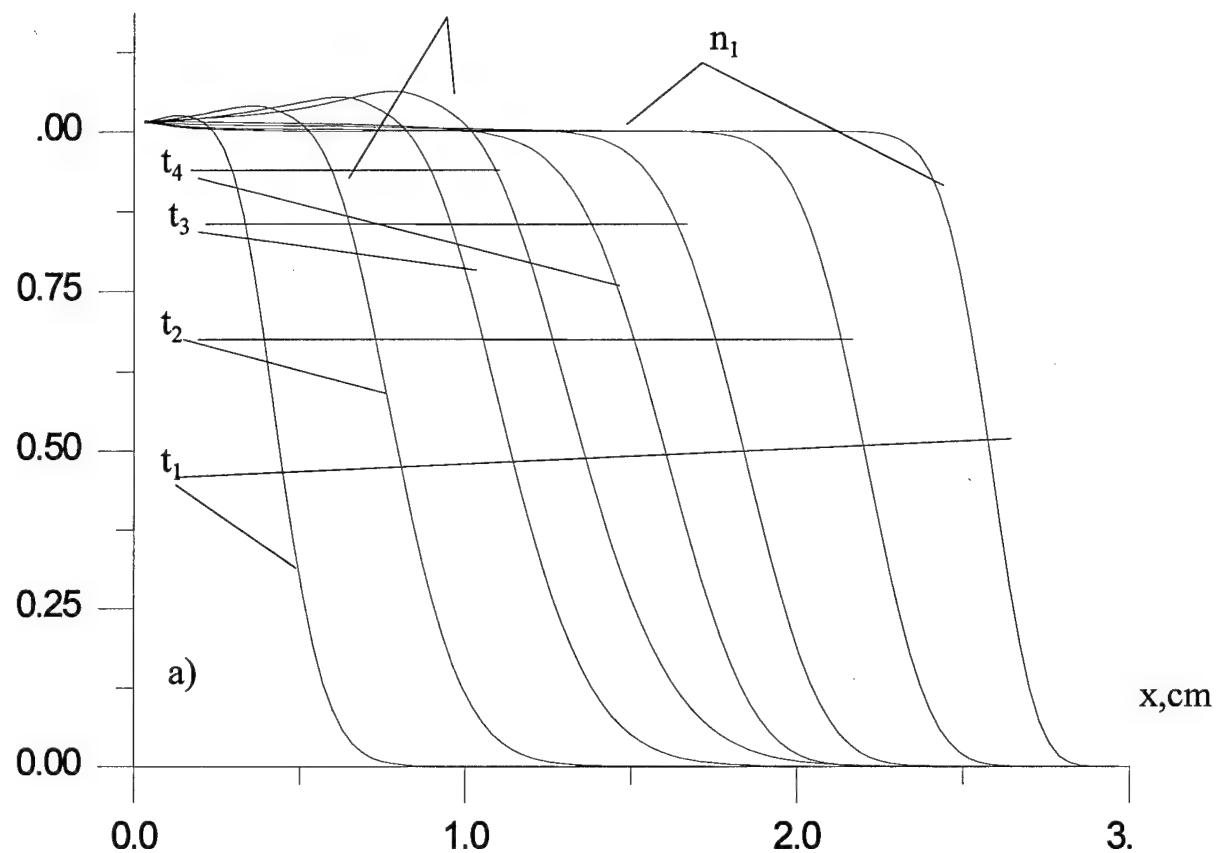
Fig.6
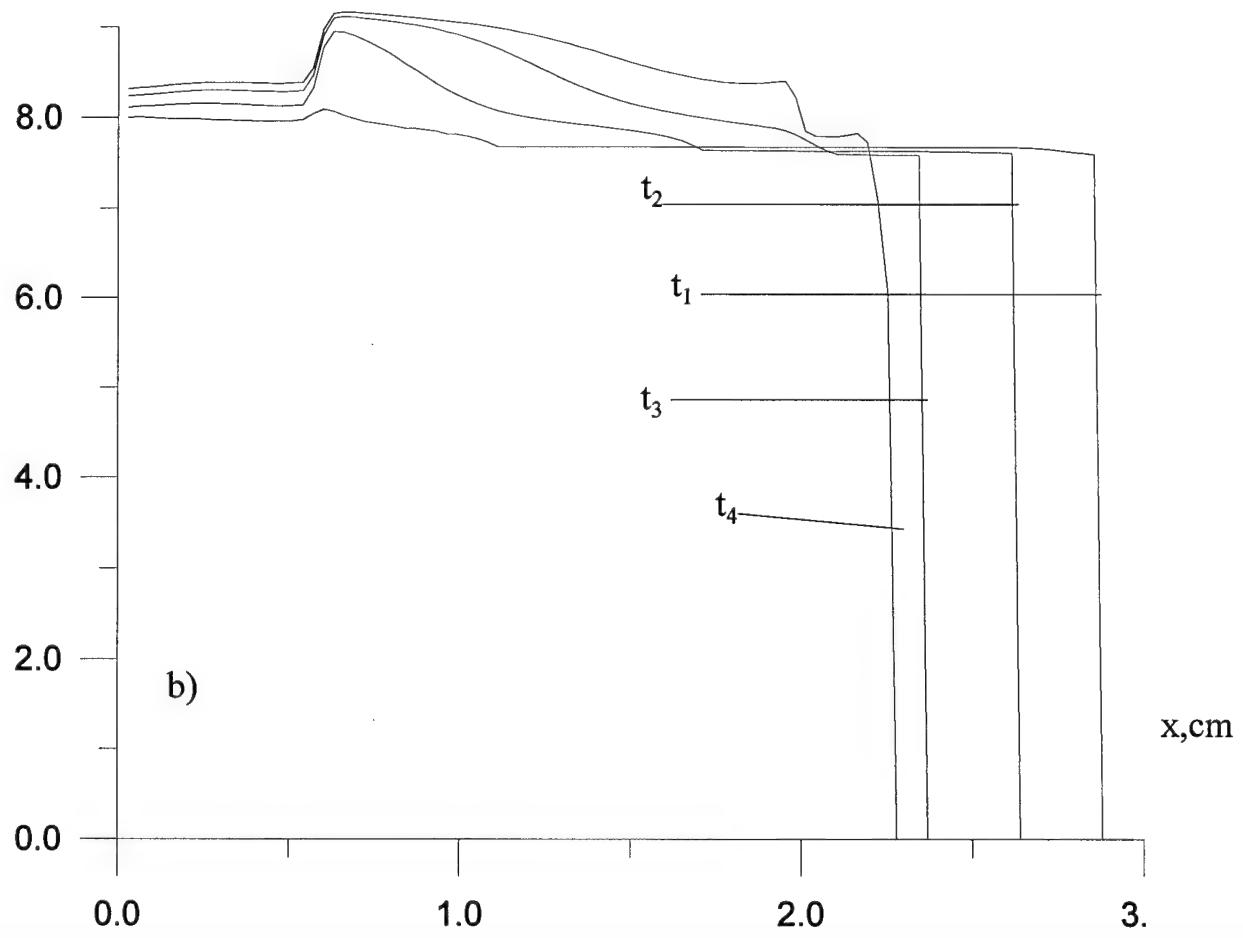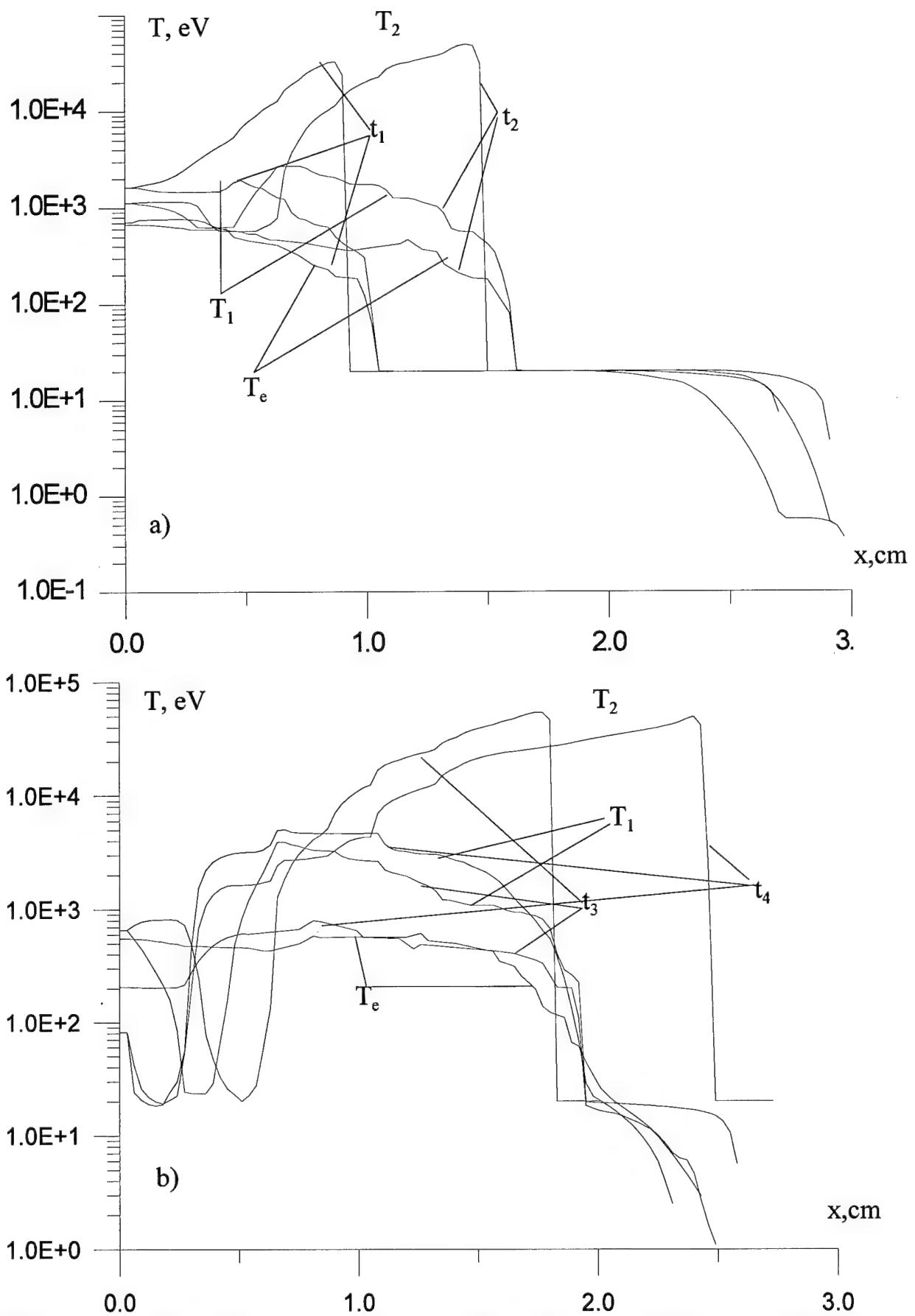
Fig.7 $n_0=10^{18}$ cm^{-3}, $R_0=3$ cm, $V_0=10^8$ cm/s, $t_1=0.138*t_x$, $t_2=0.2538*t_x$, $t_3=0.3228*t_x$, $t_4=0.4501*t_x$, $t_x=3*10^{-8}$ s

Fig.8

n*10^18 cm^-3

a)

Fig. 9

b)
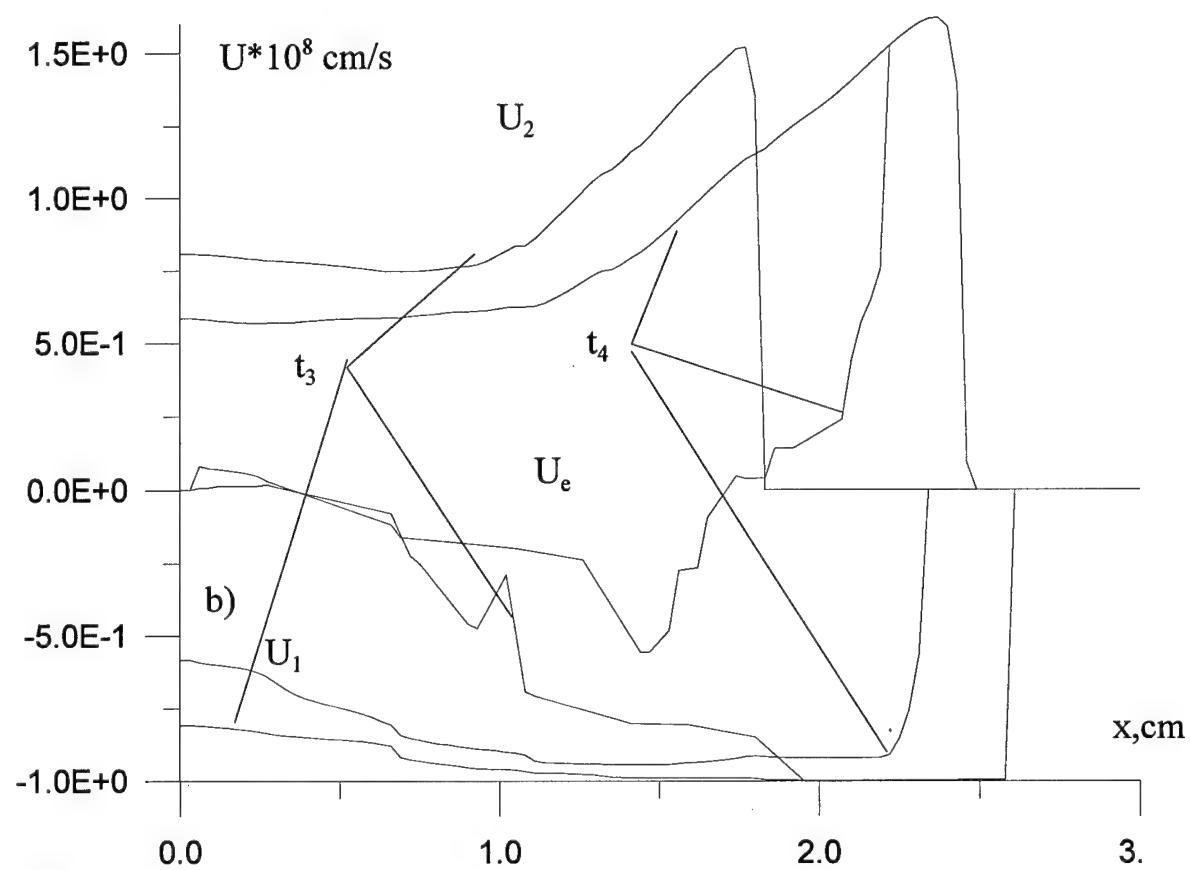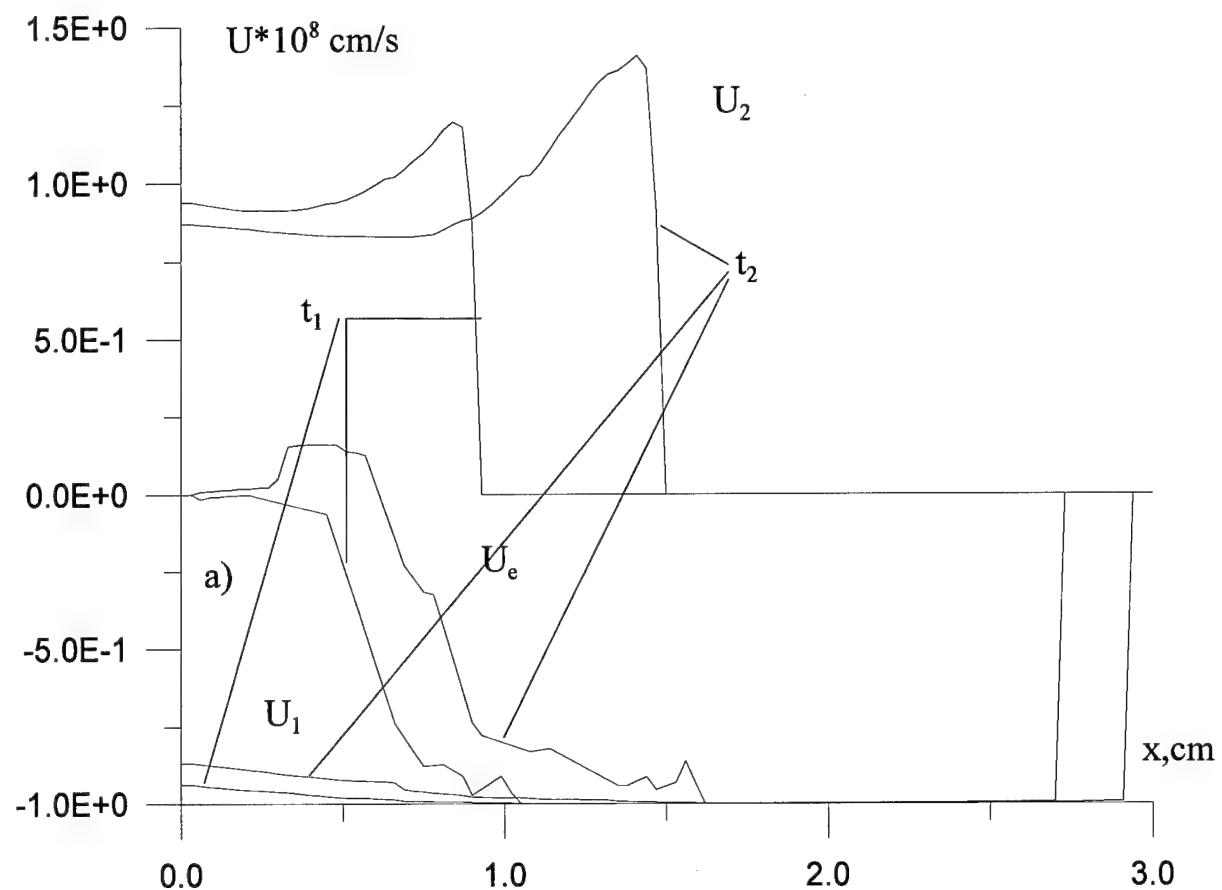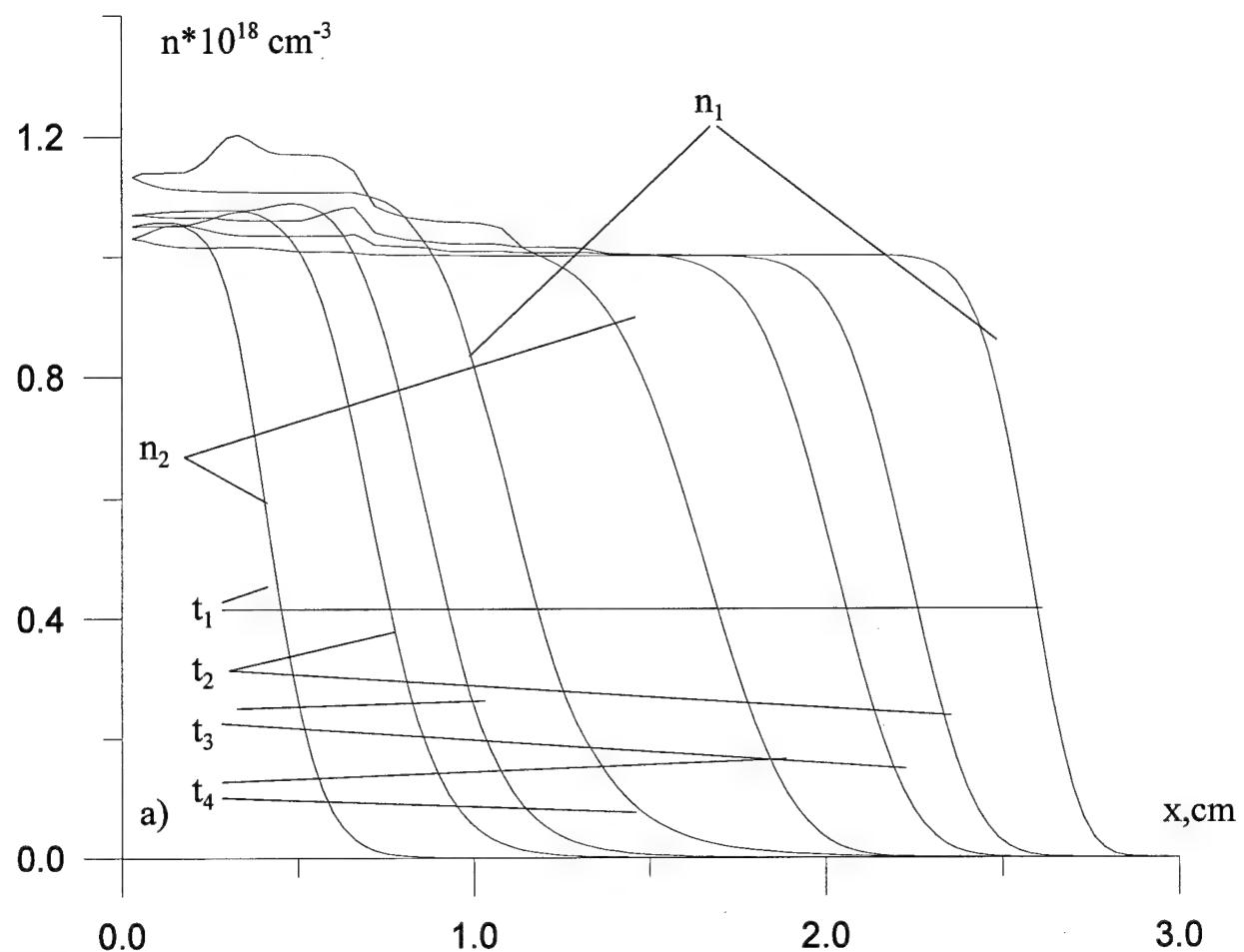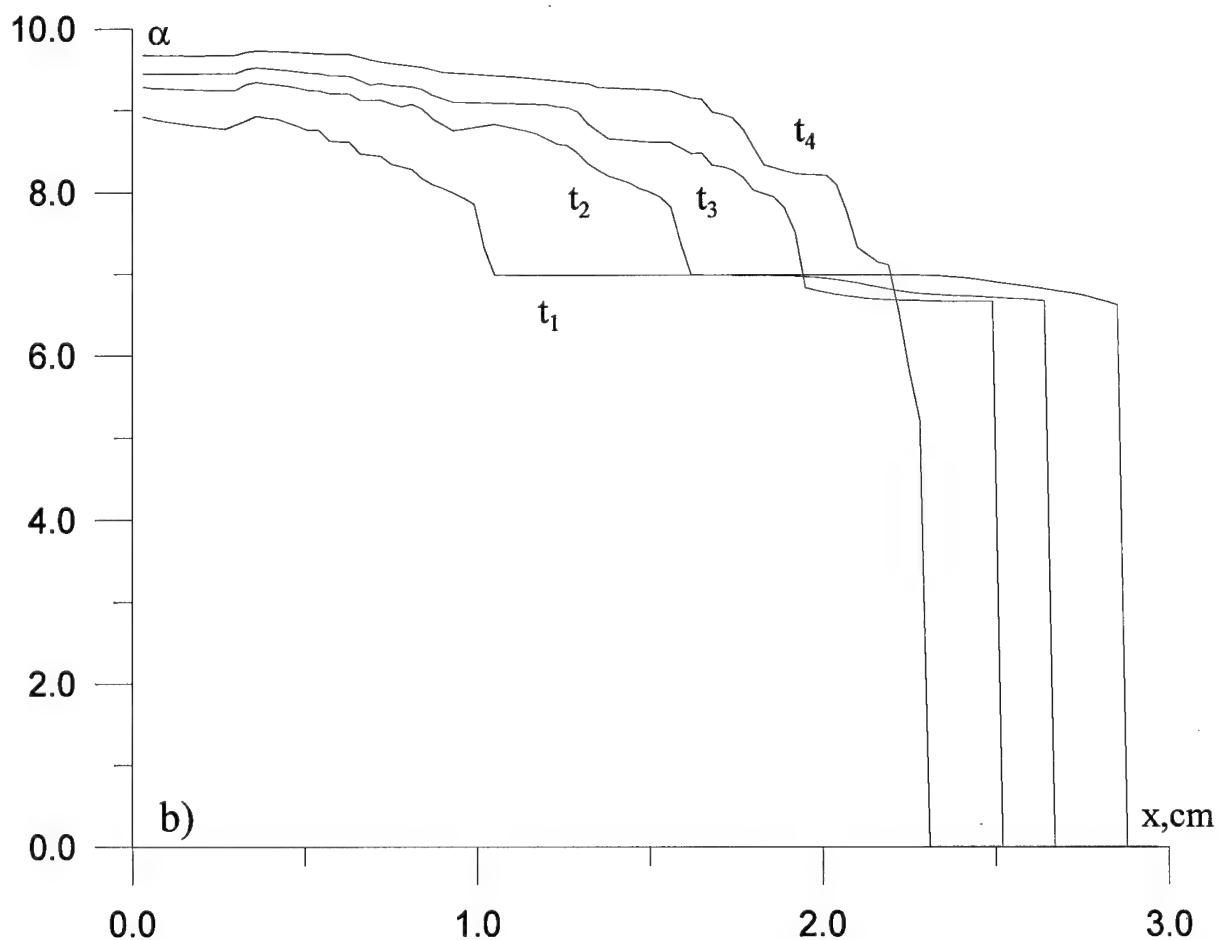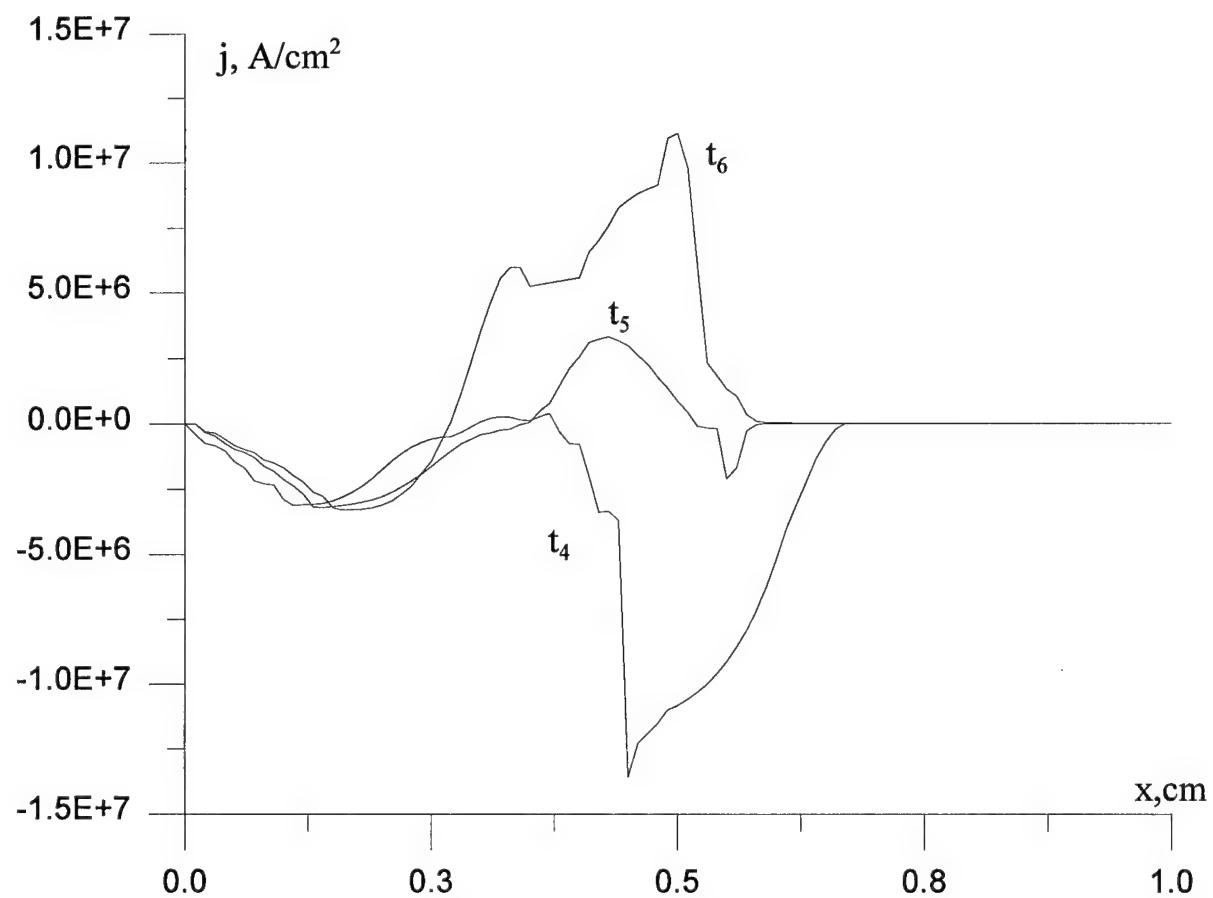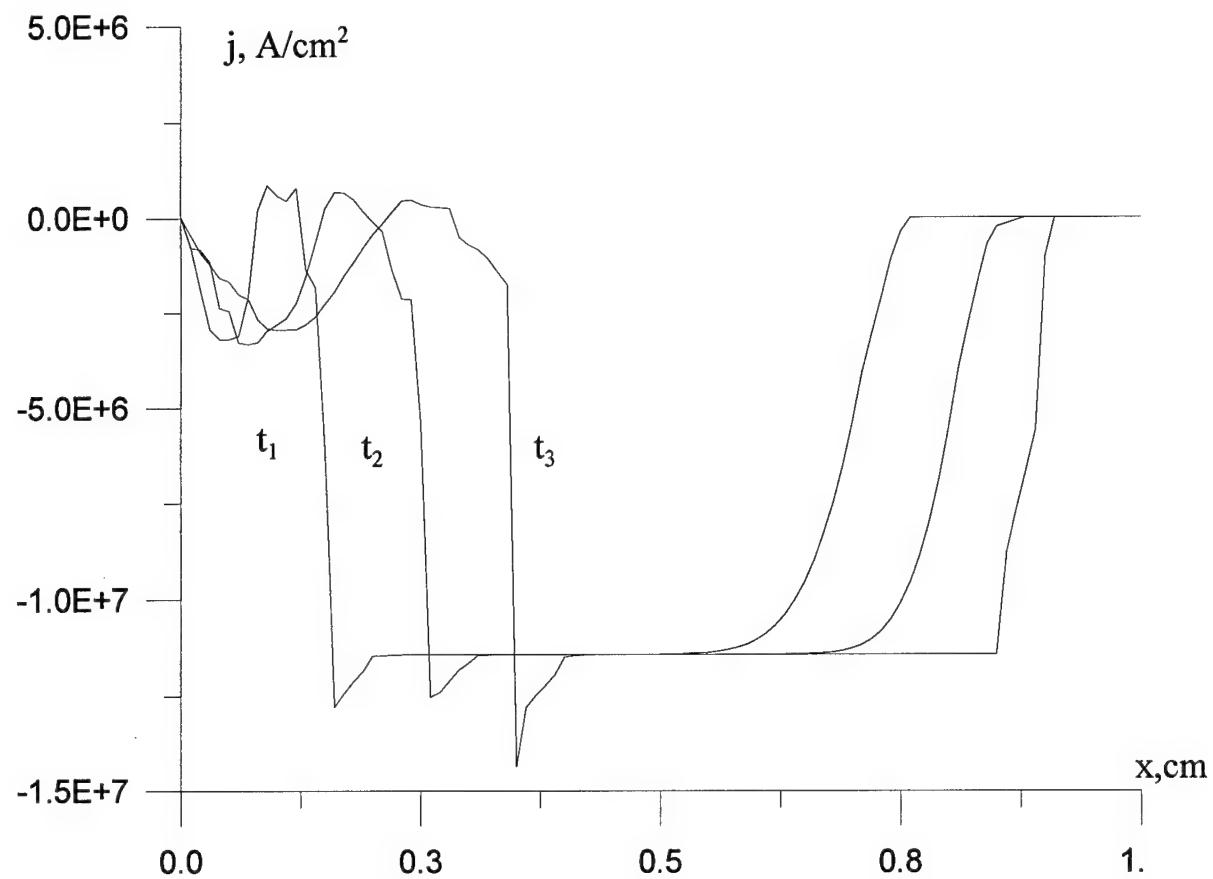
Fig.10 $n_0 = 10^{17}$ cm^{-3}, $U_0 = 10^8$ cm/s, $R_0 = 1$ cm, $t_1 = 1$ ns, $t_2 = 2$ ns, ..., $t_6 = 6$ ns
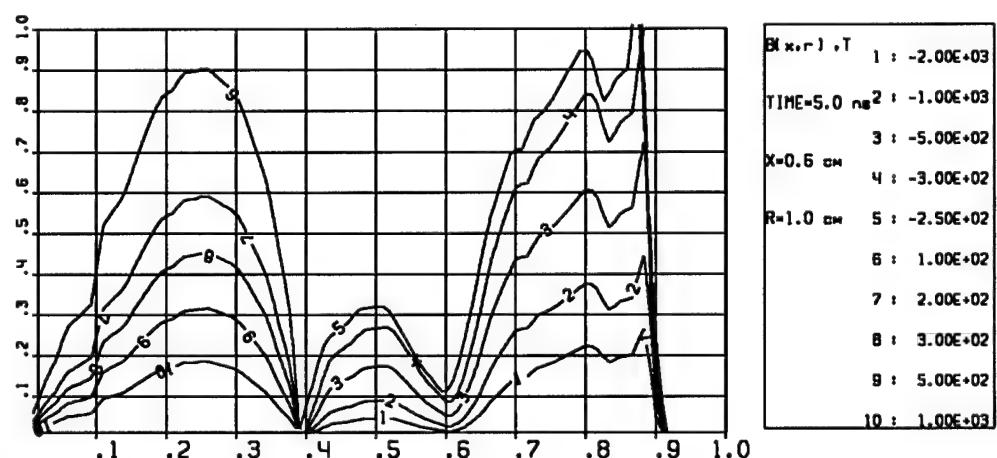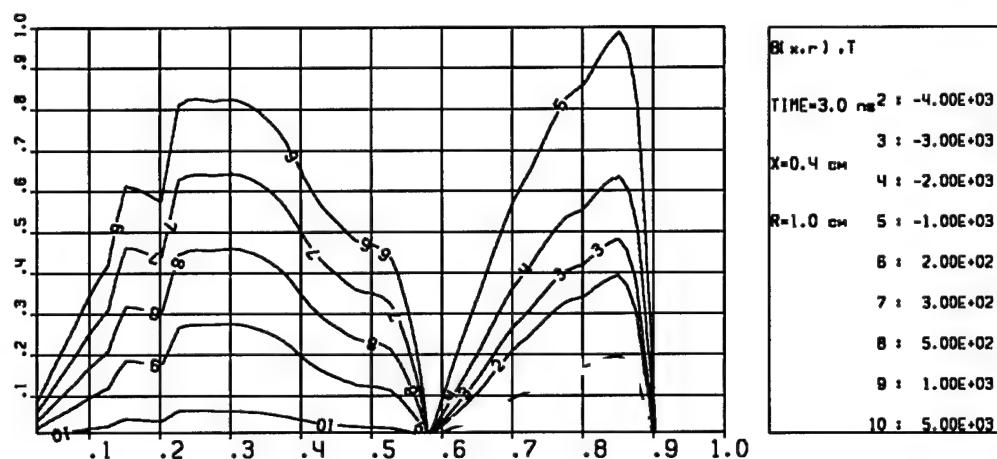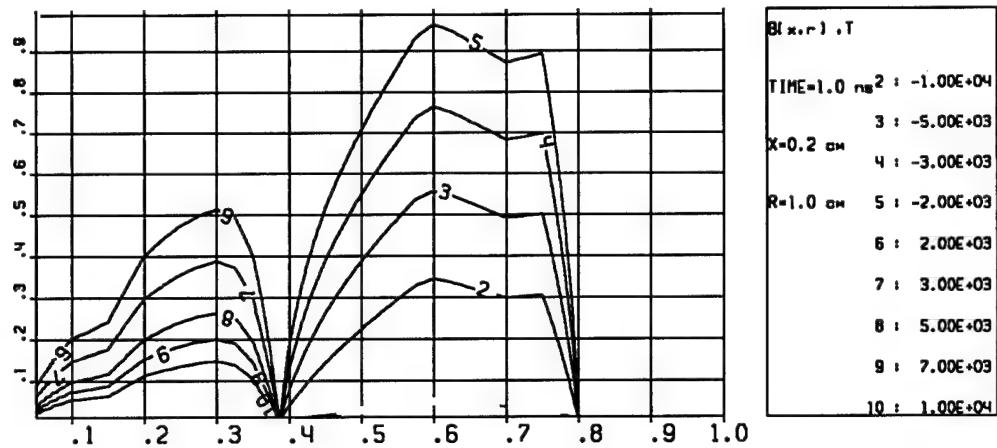
Fig. 11
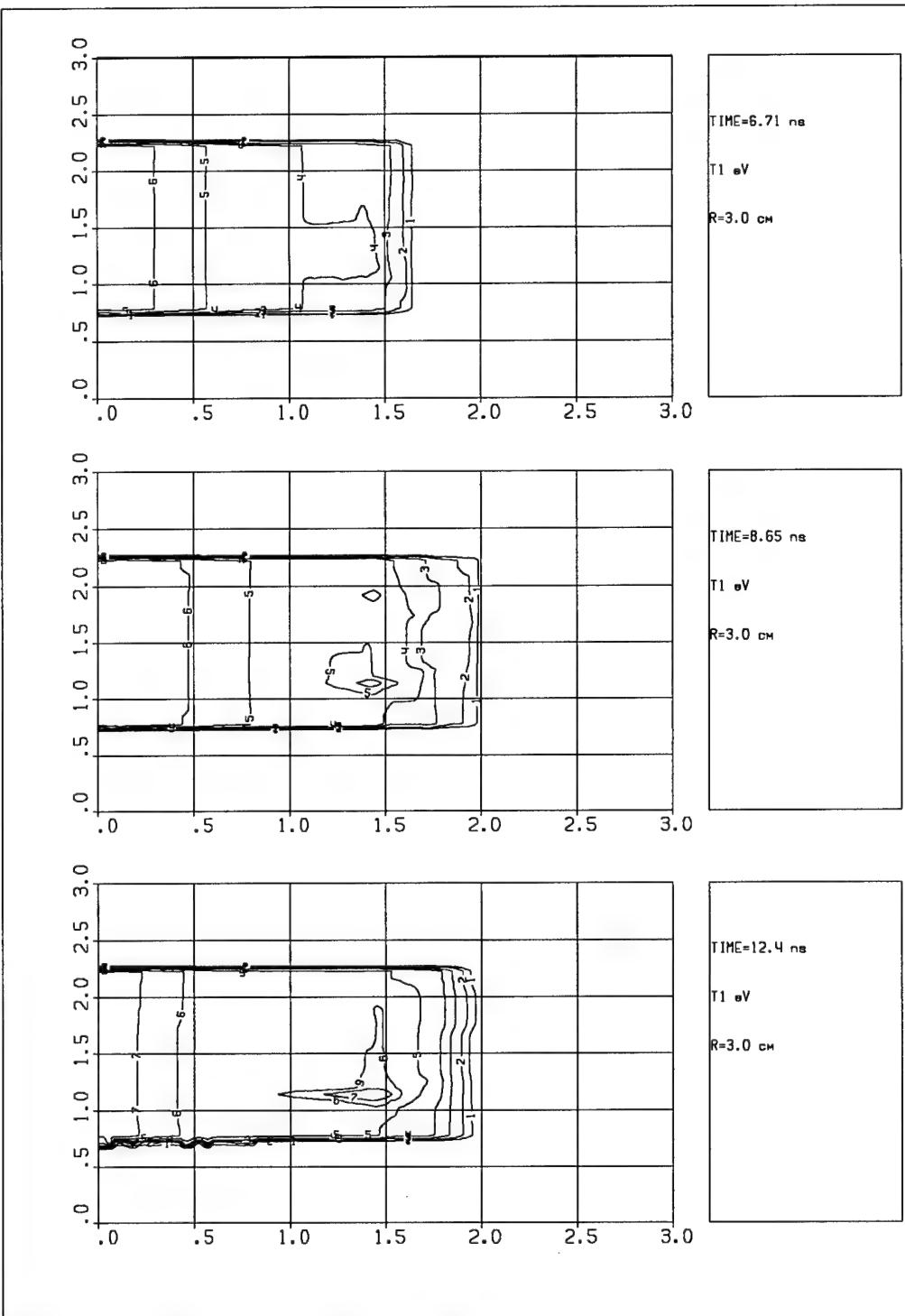
Fig.12 $n_0=10^{17}$ cm^{-3}, $U_0=10^8$ cm/s, $R_0=3$ cm

| N	T_1, eV
1	50
2	100
3	200
4	300
5	500
6	750
7	1000
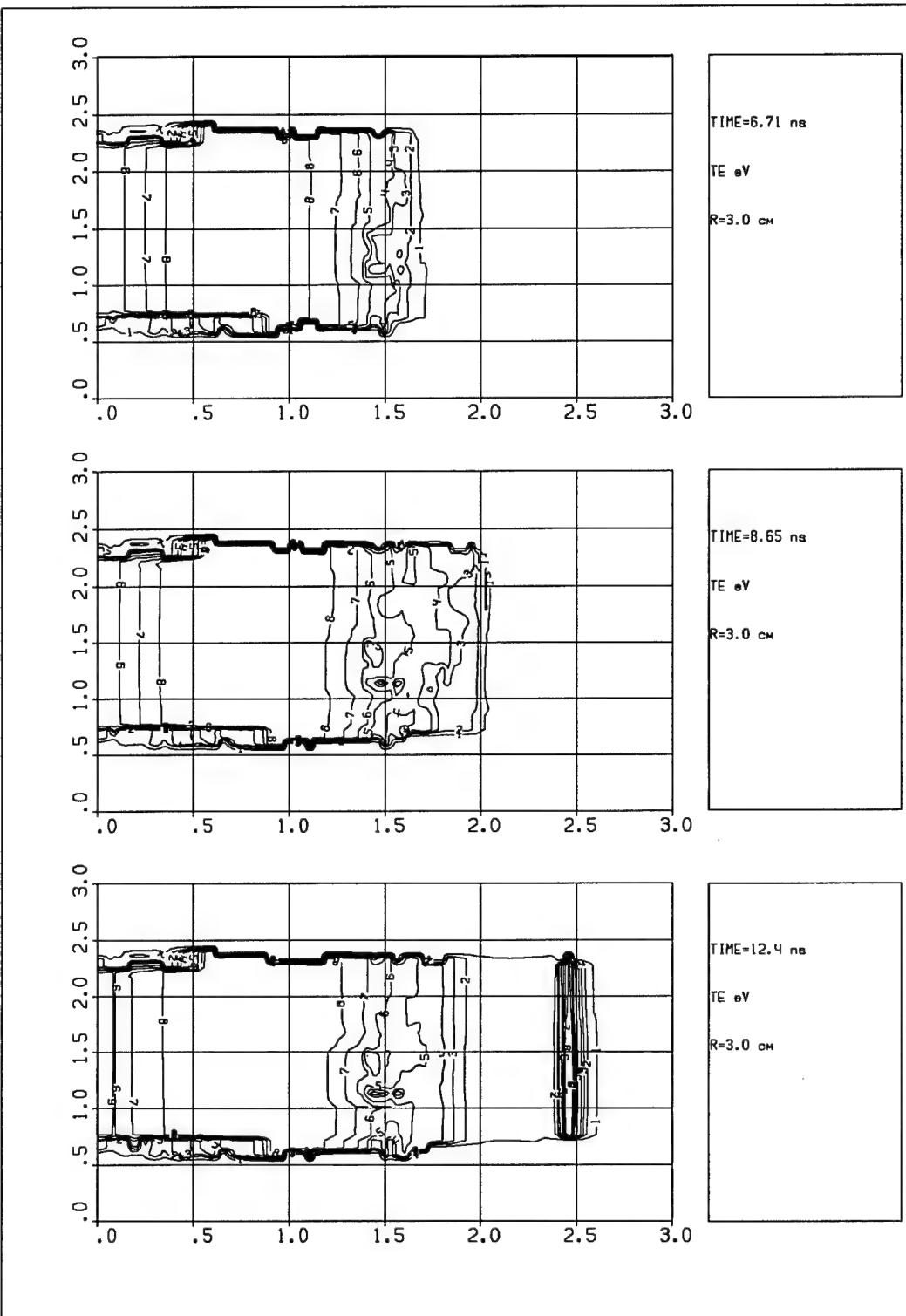
Fig.13

N	T_e eV
1	20
2	50
3	75
4	100
5	150
6	200
7	250
8	300

Panel annotations:

TIME=6.71 ns
TE eV
R=3.0 cm

TIME=8.65 ns
TE eV
R=3.0 cm

TIME=12.4 ns
TE eV
R=3.0 cm
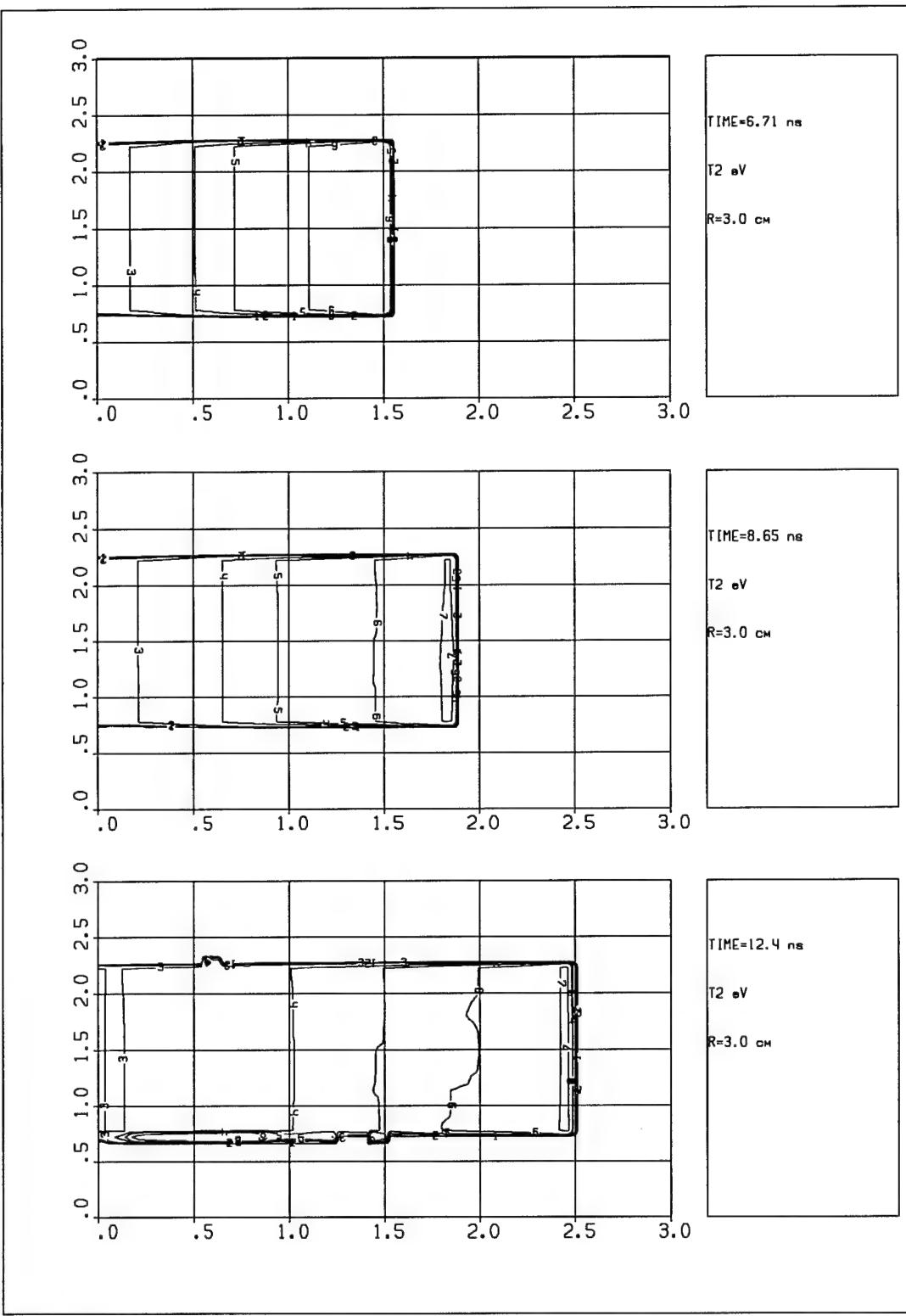
Fig. 14

| N	T_2, eV
1	300
2	500
3	1.E3
4	3.E3
5	5.E3
6	1.E4
7	3.E4
8	5.E4
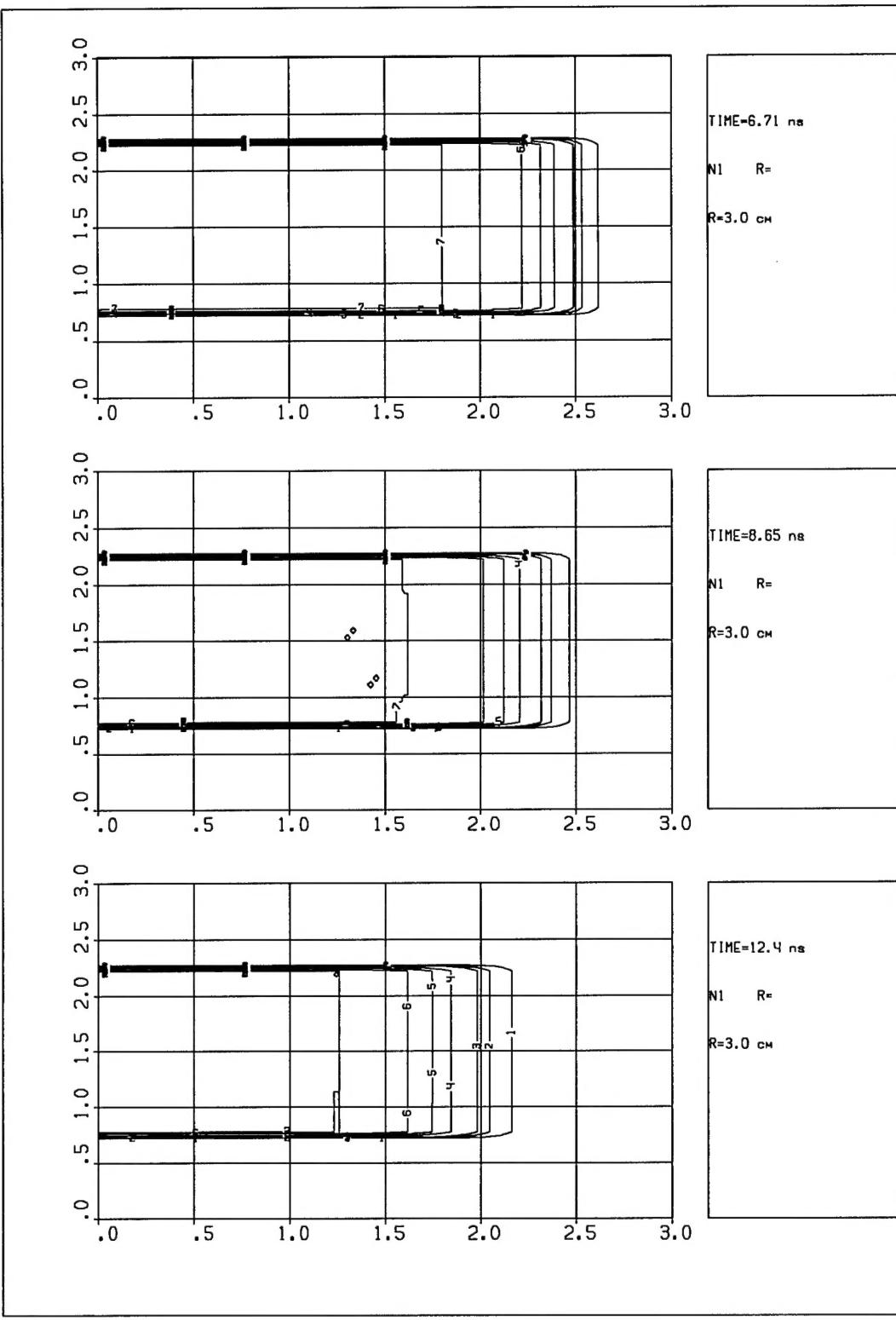
Fig. 15

N	n_1*10^{17} cm^{-3}
1	0.01
2	0.05
3	0.1
4	0.3
5	0.5
6	0.75
7	1.0

Fig.16

| N	$n_1 * 10^{17}$ cm^{-3}
1	0.01
2	0.05
3	0.1
4	0.3
5	0.5
6	0.75
7	1.0

time=6.71 ns

$\vec{U}_2$

$\longrightarrow$ - 10^8 cm/s

a)

time=8.65 ns

$\vec{U}_2$

$\longrightarrow$ - 10^8 cm/s

b)

time=12.4 ns

$\vec{U}_2$

$\longrightarrow$ -10^8 cm/s

c)

Fig. 17

time=6.71 ns

$\vec{U}_e$

→ - 10^8 cm/s

a)

time=8.65 ns

$\vec{U}_e$

→ - 10^8 cm/s

b)

time=12.4 ns

$\vec{U}_e$

→ - 10^8 cm/s

c)

Fig.18